EVOLUTION OF FLUID CHEMISTRY INSIDE A WASTE PACKAGE DUE TO CARBON STEEL AND SIMULATED HIGH-LEVEL WASTE GLASS CORROSION—PROGRESS REPORT

Prepared for

U.S. Nuclear Regulatory Commission
Contract NRC–02–02–012

Prepared by

Xihua He
Vijay Jain
F. Paul Bertetti
David Pickett

Center for Nuclear Waste Regulatory Analyses
San Antonio, Texas

January 2007

ABSTRACT

Radionuclide release from the waste package is a complex process that depends upon the corrosion rates of waste package; the chemical composition and flux of groundwater contacting the waste package internal metallic components including 304L, 316L stainless steel, and carbon steel, and the wasteforms; the dissolution rate of high-level waste glass and spent nuclear fuel; the solubility of radionuclides; the availability and stability of colloids; and the retention of radionuclides in secondary phases. Typically, the corrosion rate for carbon steel is significantly higher than for stainless steel or Alloy 22 and has a significant effect on the chemical evolution of the in-package solutions.

In this study, a series of bench-scale experiments was conducted to monitor the evolution of the chemical composition, pH, and redox potential of the fluid inside the waste package for corroding A516 carbon steel samples for expected groundwater compositions. Limited tests of neptunium sorption on corrosion products were conducted. The pH of the solution is an important parameter that controls the dissolution of wasteforms and determines the speciation of radionuclides between solid and aqueous phases. Results indicate that the corrosion processes of carbon steel in simulated J–13 or pore waters increased the pH of the solution from near-neutral to alkaline (pH >9), accompanied by the formation of iron-bearing corrosion product precipitates. The addition of simulated high-level waste glass to the corroding carbon steel solution caused a further increase in pH. These results are in contrast to the U.S. Department of Energy proposed model abstraction for in-package chemistry for Yucca Mountain in which the pH is expected to remain near neutral after initially acidic conditions (pH around 4). Carbon steel corrosion products showed substantial sorption of neptunium; however, the presence of a small amount of calcite in the corrosion products may also contribute to the sorption. The colloid content appeared to be low; however, the ability to accurately measure colloidal concentration may be limited by the resolution of the particle size analyzer used in this work. The method of identifying iron colloids needs to be improved for future studies.

CONTENTS

FIGURES

TABLES

ACKNOWLEDGMENTS

This report was prepared to document work performed by the Center for Nuclear Waste Regulatory Analyses (CNWRA) for the U.S. Nuclear Regulatory Commission (NRC) under Contract No. NRC–02–02–012. The activities reported here were performed on behalf of the NRC Office of Nuclear Material Safety and Safeguards, Division of High-Level Waste Repository Safety. This report is an independent product of CNWRA and does not necessarily reflect the view or regulatory position of NRC.

The authors gratefully acknowledge R. Pabalan for technical discussions of this work, Mr. B. Derby and S. Watson for conducting the laboratory tests, the technical review of J. Myers, the programmatic review of G. Wittmeyer, and the editorial review of L. Mulverhill. Appreciation is due to L. Naukam for assistance in the preparation of this report.

QUALITY OF DATA, ANALYSES, AND CODE DEVELOPMENT

DATA: All CNWRA-generated original data contained in this report meet the quality assurance requirements described in the Geosciences and Engineering Quality Assurance Manual. Experimental data have been recorded in CNWRA scientific notebook numbers 706, 767E, and 783. Sources for other data should be consulted for determining the level of quality for those data.

ANALYSES AND CODES: StreamAnalyzer Version 2.0 and EQ3/6 Version 7.2b codes were used for chemical speciation calculations. Geochemist's Workbench® Version 6.0 was used to simulate changes in water chemistry.

References

CNWRA. "Geosciences and Engineering Division Quality Assurance Manual." Rev. 5. 2005.

OLI Systems, Inc. "LabAnalyzer and StreamAnalyzer." Version 2.0. Morris Plains, New Jersey: OLI Systems, Inc. 2004.

Wolery, T.J. "EQ3/6, A Software Package for Geochemical Modeling of Aqueous Systems: Package Overview and Installation Guide (Version 7.0)." UCRL–MA–110662 PT I. Livermore, California: Lawrence Livermore National Laboratory. 1992.

Bethke, C.M. "The Geochemist's Workbench® Release 6.0. Reaction Modeling Guide. A User's Guide to React and Gtplot." Urbana, Illinois: University of Illinois Hydrogeology Program. 2005.

1 INTRODUCTION

The waste package, composed of metal containers and enclosed wasteforms, is the primary engineered barrier controlling the release of radionuclides from spent nuclear fuel and high-level waste glass. Penetration of the waste package by corrosion or disruptive events may allow seepage water to enter and contact the wasteforms. Because the release of radionuclides from the waste packages depends on the dissolution of cladding, spent nuclear fuel, and vitrified high-level waste, the chemistry of the aqueous environment in contact with wasteforms needs to be evaluated to assess degradation, radionuclide release, solubility limits, and colloid stability. Important parameters include the chemical composition, redox potential (Eh), and pH of the aqueous solutions contacting the wasteforms, temperature, and the formation of corrosion products from the internal components. In-package chemistry abstractions used in the U.S. Department of Energy (DOE) performance assessment should be able to estimate time-dependent wasteform degradation rates and solubility constraints and to assess the stability and concentration of colloids.

In a U.S. Nuclear Regulatory Commission (NRC) evaluation of the risk significance of postclosure performance assessment model abstractions (NRC, 2004a), staff provided the basis for the importance of specific abstractions affecting radionuclide release rates and solubility limits. The conclusions of NRC (2004a) reflected the relevance to performance of the in-package environment as discussed in the preceding paragraph. Four aspects of the relevant DOE abstractions (Bechtel SAIC Company, LLC, 2004a,b) were concluded to have medium significance to waste isolation: wasteform degradation rate, cladding degradation, solubility limits, and the effect of colloids on waste package releases.

This report documents the status of ongoing, independent efforts by the Center for Nuclear Waste Regulatory Analyses (CNWRA) to evaluate the DOE in-package chemistry abstraction. The majority of this work has involved laboratory experiments on water chemistry evolution in the presence of potential waste package components, chiefly A516 carbon steel. Experiments on radionuclide sorption on carbon steel corrosion products, which is a process invoked in the DOE performance assessment to slow release from the waste package (Bechtel SAIC Company, LLC, 2004c) are also discussed. Preliminary efforts to perform independent modeling of in-package chemistry evolution are also discussed.

1.1 Objectives

Key objectives of this study are to (i) experimentally determine the evolution of the chemical composition, pH, and redox potential of the fluid inside the waste package for corroding carbon steel samples for expected groundwater compositions; (ii) experimentally determine sorption of neptunium on iron corrosion products; and (iii) conduct simulations to predict the evolution of pH of the fluid inside the waste package for corroding carbon steel samples for expected groundwater compositions.

1.2 Organization of the Report

This report is organized into five chapters, including the introduction as Chapter 1. The in-package chemistry abstraction is discussed in Chapter 2. The experimental details are given in Chapter 3. The results and discussions are given in Chapter 4. Chapter 5 provides the summary, conclusions, and future work.

2 ABSTRACTING IN-PACKAGE CHEMISTRY

2.1 U.S. Department of Energy Approach to In-Package Chemistry

The U.S. Department of Energy (DOE) in-package chemistry model was based on two specific waste packages—a waste package containing commercial-spent nuclear fuel and a codisposal waste package containing DOE-spent nuclear fuel and high-level waste glass (Bechtel SAIC Company, LLC, 2004a,b). These two package types were considered representative of all waste packages in the repository. By varying input parameters to account for a range of system properties, environmental properties, and material properties, the in-package chemistry model simulates interactions of water with the specified waste package components under different physical, hydrological, and chemical conditions. DOE stated that the exact pathway infiltrating or condensing water would follow within the waste package is unknown, but it is very unlikely that water would contact only the fuel and bypass the other materials inside the waste package.

In developing the in-package chemistry abstraction, DOE used two modeling approaches to simulate chemical changes over time inside a waste package—a physical chemistry model and a surface complexation model. The main modeling approach in the in-package chemistry abstraction was a physical chemistry model applied in two stages. First, the model was used to simulate kinetic reactions between incoming water and individual waste package components, calculating the contribution of each to waste package chemistry. Second, the model was applied to a more complex environment to simulate kinetic reactions between incoming water and a combination of waste package components, including the wasteforms themselves, and determine how coupled reactions affected the evolution of the in-package chemistry. The physical chemistry model was implemented with the reaction-path software code EQ3/6 for a range of specified conditions inside a waste package. The input parameters that were varied included system properties (water distribution and mode of occurrence inside the waste package), environmental properties (temperature, carbon dioxide gas partial pressure, and water flux rates), and material properties (composed of waste package components and of the incoming water, degradation and corrosion rates, and masses and surface areas of reactants). Among the values calculated by EQ3/6 were the effluent pH, ionic strength, redox conditions, and the concentrations of dissolved species such as carbonate and fluoride. These properties are important because they provide direct or indirect input to the submodels that simulate wasteform degradation, radionuclide solubility limits, and colloid concentrations.

The second modeling approach DOE used was a surface complexation chemistry model, described as an analytic derivation of pH, that was applied separately from the physical chemistry model. The physical chemistry model predicted that, under certain conditions, the steel corrosion could result in very low pH values inside the waste package. In the waste package chemical environment as a whole, however, surface complexation reactions (protonation) involving steel corrosion products would tend to buffer any acidic pH conditions to a more moderate pH range of approximately 7–8. Because of an EQ3/6 software limitation, surface chemistry processes could not be coupled to the other reactions in the physical chemistry model. Instead, the surface chemistry model was applied separately to predict the in-package pH during the first 600 years after waste package breach when corrosion of Type 516A carbon steel would largely dominate the in-package chemistry. This approach appears supported by an experimental study conducted by Zarrabi, et al. (2003) on a miniature

steel waste package with carbon steel internals subjected to corrosion in J–13 Well water, where the pH of the in-package solution remained steady at around 8 during the 5-week experiment.

For the physical chemistry model, the DOE validation was based on a broad comparison of the modeled predictions with analogous systems for which similar conditions and processes have been observed (Bechtel SAIC Company, LLC, 2004a,b). This validation procedure was used to (i) confirm that the model predicted the formation of a realistic set of secondary solids by corrosion of steel and other metals in the waste package and (ii) more generally to assess that the range of pH values predicted by the model compared appropriately with the natural waters and a few laboratory experiments. Several important outputs of the EQ3/6 calculations, including the calculated ranges of ionic strength, carbonate, and fluoride concentrations, and the role of schoepite dissolution in buffering pH values, apparently were not assessed by model validation. The U.S. Nuclear Regulatory Commission (NRC) staff considered the key technical issue agreements concerned with in-package chemistry to be complete, but suggested that DOE strengthen the model validation and noted that in any potential license application NRC staff would expect DOE to provide more detailed information supporting their models (NRC, 2004c).

The surface chemistry model was validated by an independent expert technical review that concluded the approach was reasonable (Bechtel SAIC Company, LLC, 2004b, Appendix E); however, insufficient supporting information was provided to determine whether the validation of the surface complexation model is indeed complete.

DOE argued that although reactions with some of these individual waste package components may lead to local pH variations (e.g., pH <3 or >10), other and more abundant reactants in the waste package would tend to buffer the extreme pH toward more neutral values, regardless of the path followed by the water moving through the waste package. In particular, the secondary uranium mineral schoepite (a likely corrosion product of spent nuclear fuel) and iron corrosion products were identified as important solid phases that would resist deviations to high or low pH in the system. Although reaction of water with steel alone would lead to potentially large decreases in pH, the acidity could be buffered by sorption of hydrogen ions onto corrosion product surface sites [e.g., ferrihydrite ($5Fe_2O_3 \bullet 9H_2O$) or goethite ($FeO \bullet OH$)] and by dissolution of schoepite ($UO_3 \bullet 2H_2O$). Corrosion of waste glass might lead to high pH, but DOE argued this would also be buffered by schoepite dissolution. Details of these processes were discussed in the in-package environment technical basis document (Bechtel SAIC Company, LLC, 2004a, Section 3) and in a report on the in-package chemistry abstraction (Bechtel SAIC Company, LLC, 2004b).

On the basis of simulations in Bechtel SAIC Company, LLC (2004b), DOE concluded that the compositions of fluids resulting from in-package chemical reactions are largely insensitive to the initial composition of seepage water entering the package. A sensitivity study investigated three starting ambient water compositions: calcium-pore water, sodium-pore water, and J–13 Well water. The pore water values were taken from site data. The sensitivity study also employed three thermally perturbed water compositions representing a range of carbon dioxide fugacity and temperature conditions, abstracted from Bechtel SAIC Company, LLC (2004d). The results from the two sets of calculations—involving both ambient and thermally perturbed waters—showed that pH and ionic strength vary little with input water chemistry (e.g., Bechtel SAIC Company, LLC, 2004a, Figures B–1 and B–2). DOE neglected the potential effect of

high-ionic-strength solutions that could develop due to evaporative concentration on the basis that evaporation would also substantially decrease the amount of seepage water that could enter the waste package while the waste package is hot.

The NRC staff agrees with the DOE conclusion that chemical interactions of water with in-package components will dominate the changes in chemistry of in-package water. The NRC staff considers the DOE rationale for neglecting the potential effect of high-ionic-strength solutions to be appropriate.

In summary, the general DOE approach to abstracting in-package chemistry appears sound. Some questions remain, however, regarding the detailed basis and validation of the underlying process models.

2.2 Preliminary Center for Nuclear Waste Regulatory Analyses Modeling

Because of uncertainties in in-package chemistry modeling and NRC questions regarding DOE models and their validation (NRC, 2004b,c), independent analyses designed to evaluate the results of DOE in-package chemistry models by constructing similar models using different tools and approaches are underway at the Center for Nuclear Waste Regulatory Analyses (CNWRA). The models are also being used to better understand aqueous chemical evolution during CNWRA steel corrosion experiments (Chapters 3 and 4). These models are being developed using Geochemist's Workbench® Version 6.0 software. Initial efforts have used the React component of Geochemist's Workbench® to simulate changes in water chemistry (starting composition approximating J–13 Well water) as steel and spent fuel elemental components are added to solution. The default "thermo.dat" thermodynamic database was employed and default model conditions include the starting CNWRA experimental solution composition (e.g., pH = 8.34), temperature of 60 °C [140 °F], atmospheric control of oxygen and carbon species. Input parameters and conditions are being varied to help identify processes responsible for CNWRA laboratory results and to evaluate the DOE approach to bounding chemical evolution.

The first models showed a decrease in pH from the starting value of 8.34 to 5.5, with a decreasing trend resulting from sulfate addition on oxidation of steel-derived sulfur. This trend agrees with DOE physical chemistry model predictions but contrasts with the increasing pH observed in CNWRA laboratory experiments (Section 4.1 in Chapter 4). A pH increase could only be achieved by allowing oxygen to be consumed by imposing a closed system (Log f_{O2} decreasing to −47) or by removing nitrate from the basis entry list. In this case, pH approached a steady-state value of 9.6—similar to the CNWRA experimental results. A mechanism (aside from imposing less oxidizing conditions) that prevents sulfur oxidation from lowering the pH in the starting solution has not been identified.

Simulations have also included equilibration of uraninite (spent nuclear fuel analogue) and schoepite in the solution with and without steel components. Uraninite had little effect on solution pH, presumably due to its very low solubility. Schoepite, however, when equilibrated in the absence of steel, imposed a pH of 7.7. This is generally consistent with the DOE assertion that schoepite will influence pH to remain in the near-neutral range (Bechtel SAIC Company, LLC, 2004b). When combined with steel components, an increasing proportion of schoepite moves the solution pH from 9.6 toward 7.7 (e.g., a schoepite/steel ratio of 6 yielded pH = 8.25).

In summary, the models have not yet helped to identify the pH-controlling mechanism in our experiments. However, key aspects of the DOE in-package physical chemistry model have been identified, namely, low pH resulting from sulfur oxidation on carbon steel dissolution (noting that this mechanism is not ultimately used in their abstraction) and near-neutral pH resulting from schoepite equilibration. This model-to-model comparison is limited with respect to validation of the DOE results. Comparisons with laboratory results and natural systems would improve the DOE validation.

Sensitivity analyses of the model results will help pinpoint the components and mechanisms that are influencing pH evolution during the CNWRA experiments. In addition, by replacing carbon steel with stainless steel in the simulations, the detailed chemical effects of potential waste package design changes can be investigated.

3 EXPERIMENTS

The experimental details include carbon steel and simulated high-level waste glass immersion in simulated groundwaters and radionuclide sorption on carbon steel corrosion products.

3.1 Carbon Steel and Glass Immersion Experiments

3.1.1 Preparation of Test Waters

Simulated J–13 Well water and simulated sodium-pore water were selected as the starting ambient waters. Each simulated water was prepared from two stock solutions, A and B, listed in Table 3-1. Before use, equal amounts of stock solutions were mixed and diluted fortyfold to prepare the simulated waters. Table 3-2 lists the calculated and analyzed chemical compositions and pH of the simulated J–13 Well water and simulated sodium-pore water along with input chemical composition of J–13 Well water and sodium-pore water used in the U.S. Department of Energy (DOE) model calculation (Bechtel SAIC Company, LLC, 2004a). The calculated chemical compositions are in agreement with what was analyzed. Except for pH, the chemical compositions of the test waters are very similar to the input chemical compositions used by DOE. The difference in pH could be due to the difference in CO_2 pressure in on-site J–13 Well water and in the laboratory.

3.1.2 Materials and Test Cells

A516 carbon steel and simulated SRS–202G high-level waste glass of chemical compositions listed in Table 3-3 were used in the immersion tests. The carbon steel specimens with dimensions about 1.27 cm × 1.27 cm × 0.5 cm [0.5 in × 0.5 in × 0.2 in] were wet polished with a 600-grit sand paper finish, rinsed with high-purity water, and cleaned with acetone. The simulated high-level waste glass was provided as discs {1-cm [0.4-in] diameter and 1.5 mm [59 mil] thick} with a surface area of 2 cm^2 [0.3 in^2]. The glass discs were cleaned with acetone before use.

The immersion tests were conducted in two types of test cells: 60-mL [2.0-oz] polytetrafluoroethylene vessels and 250-mL [8.45-oz] glass cells with polytetrafluoroethylene lids. In later tests, the glass test cells were lined with polytetrafluoroethylene liner to avoid glass dissolution. The glass test cells were fitted with a water-cooled condenser to minimize solution loss at elevated temperatures. The test cell was open to air through the condenser. The carbon steel and glass samples were suspended in the center of the test cell on a polytetrafluoroethylene crater. To simulate an internal waste package environment, the ratio of the test water volume to the surface area of A516 carbon steel was 13.7 mL/cm^2 [2.99 oz/in^2], which is the ratio of the void volume inside the waste package {4,594 L [1,212 gal]} (Bechtel SAIC Company, LLC, 2001) to the surface area of carbon steel {334,300 cm^2 [51,817 in^2]} (Bechtel SAIC Company, LLC, 2004b, Table 6-11) available in the waste package. In one test, the carbon steel specimen was threaded and connected to a stainless steel rod to allow electric contact for monitoring corrosion potential of carbon steel in solution. The connecting joint of carbon steel and the stainless steel rod was wrapped with polytetrafluoroethylene tape. For this test cell, a saturated calomel electrode was used as a reference, and it was connected to the

Table 3-1. Stock Solutions A and B for Simulated Water Preparation				
Target Waters	**Stock Solution A**		**Stock Solution B**	
	Chemical Reagents	**Concentration (g/L*)**	**Chemical Reagents**	**Concentration (g/L*)**
Simulated J–13 Well Water	$CaSO_4 \cdot 2H_2O$	1.374	$NaHCO_3$	6.720
	$Ca(NO_3)_2 \cdot 4H_2O$	0.942		
	KCl	0.116	$KF \cdot 2H_2O$	0.379
	$MgCl_2 \cdot 6H_2O$	0.570		
Simulated Sodium-Pore Water	$CaSO_4 \cdot 2H_2O$	2.245	$NaHCO_3$	16.487
	$Ca(NO_3)_2 \cdot 4H_2O$	0.032		
	KCl	0.47		
	$MgCl_2 \cdot 6H_2O$	1.129	NaF	0.544
	$CaCl_2$	0.726		
*1 g/L = 8.35×10^{-3} lb/gal				

solution through a water-cooled Luggin probe with a porous silica tip to maintain the reference electrode at room temperature. The solution used in the Luggin probe is the same as that used in the test cell.

Most of the tests were carried out at 60 °C [140 °F], with the exception of one test conducted at 90 °C [194 °F]. The glass test cell was heated from the outside by heating strips. The temperature was maintained by a temperature controller and measured by a thermocouple. The glass thermowall in contact with solution was wrapped with polytetrafluoroethylene tape to avoid glass dissolution. For tests conducted in polytetrafluoroethylene vessels, the vessels were kept in an oven to maintain constant temperature.

3.1.3 pH Monitoring and Solution for Chemical Composition Analysis

During tests, the solution pH was monitored using a pH meter with a standard-sized glass body combination electrode. Each time, 1 mL [0.03 oz] of test solution was drawn for chemical composition analysis. For tests in simulated sodium-pore water, after 1 mL [0.03 oz] of solution was drawn, 1-mL [0.03-oz] fresh original pore water was added to compensate for solution volume changes. The anions were analyzed using the ion chromatography method, and the cations were analyzed using the inductive coupled plasma method.

Table 3-2. Chemical Composition of Simulated Waters						
	Simulated J–13 Well Water			Simulated Sodium-Pore Water		
Species	Calculated (mg/L*)	Analyzed by inductive coupled plasma method (mg/L*)	DOE Used (mg/L*)†	Calculated (mg/L*)	Analyzed by inductive coupled plasma method (mg/L*)	DOE Used (mg/L*)†
Ca^{2+}	12.0	12.0	13.0	18.1	17.3	41
K^{+}	5.47	<12.5	5.04	6.16	<7.50	6.1
Mg^{2+}	1.70	<2.50	2.01	3.37	3.32	3.3
Na^{+}	46.0	44.0	45.8	120	119	120
SO_4^{2-}	19.2	18.8	18.4	31.3	31.0	31
NO_3^{-}	12.4	N/D‡	8.78	0.42	<1.00	0.41
Cl^{-}	6.33	N/D‡	7.14	24.2	22.9	24
F^{-}	1.92	N/D‡	2.18	6.15	5.68	6
HCO_3^{-}	122	N/D‡	Calculated From Charge Balance	299	N/D‡	362
Measured pH	8.34		7	8.48		7.4

*1 mg/L = 8.35×10^{-6} lb/gal
† (Bechtel SAIC Company, LLC, 2004b)
‡ N/D = Not Determined

3.1.4 Corrosion Product Characterization

The corrosion products were characterized with several techniques including particle size distribution analyzer and environmental-scanning electron microscopy for particle size distribution analysis, scanning electron microscopy and energy dispersive x-ray spectroscopy for chemical composition analysis, and x-ray diffraction and Raman spectroscopy for *ex-situ* identification of mineral phases. Environmental scanning electron microscopy is a new innovation in scanning electron microscopy specifically designed to study wet, oil bearing, or insulating materials without prior specimen preparation or gold coating. Samples may be examined in water vapor or other gases such as CO_2 or N_2 at near atmospheric pressures due to the unique vacuum system of the environmental scanning electron microscope. Two particle size analyzers in the submicron (using photon correlation spectroscopy) and micron (using optical counting) ranges were used. The particle size analyzer was calibrated with standard particles before use. The Raman system used a 532-nm [0.0209-mil] laser with a 63.5-mm [2,500-mil] focal-length fiberoptic bead. A power of 2 mW was chosen to prevent oxidation of Fe(II) species. Identification of corrosion products with Raman spectroscopy was performed by comparing the spectra to known compounds (Dunn, et al., 2000).

Table 3-3. Chemical Composition of A516 Carbon Steel (Weight Percent)										
A516 Carbon Steel (Heat D84944)	Fe	Si	P	Cr	Al	Mn	S	Mo	V	C
	98.74*	0.30	0.011	0.02	0.021	0.90	0.011	<0.01	<0.01	0.18

SRS-202G Simulated High-Level Waste Glass	
Oxide Compound	**Weight Percent**
Al_2O_3	5.81
B_2O_3	10.32
BaO	0.03
CaO	1.08
Cr_2O_3	0.41
CuO	0.12
Fe_2O_3	9.27
K_2O	3.28
La_2O_3	0.02
Li_2O	3.44
MgO	1.70
MnO_2	1.54
MoO_3	0.01
Na_2O	15.33
Nd_2O_3	0.01
NiO	0.95
P_2O_5	0.32
PbO	0.04
SiO_2	44.46
SnO	0.02
TiO_2	0.13
UO_3	1.61
ZnO	0.01
ZrO_2	0.08

*Based on mass balance

After testing, the carbon steel and glass specimens were cleaned with high-purity water and acetone and dried in air. The corrosion products precipitated in solution were collected and dried in air. Subsequently, the corrosion products that remained on the carbon steel surface and that were collected from solution were characterized by x-ray diffraction and scanning electron microscope. After surface analysis, the carbon steel specimens were descaled further using dilute HCl solution for 30 seconds. The weight loss was used to calculate the corrosion rate.

3.2 Neptunium Sorption Experiments

Radionuclides may attach to carbon steel corrosion products (e.g., iron oxyhydroxides) produced by the degradation of carbon steel components within waste packages. Iron oxyhydroxides have a high sorption affinity for many metals, some of which occur on radionuclide isotopes in the waste package (Dzombak and Morel, 1990). As a preliminary test of the capability of carbon steel corrosion products to sorb neptunium, a potentially important contributor to dose at long timeframes, batch sorption experiments were conducted using the carbon steel corrosion products and solutions produced in the test cells described in Section 3.1.2.

Solutions and carbon steel corrosion products from test cells run in parallel were combined in a 1-L [0.26-gal] glass beaker. A 10-mL [0.34-oz] Oxford pipettor was used to withdraw and transfer solution and corrosion products from the glass beaker to pre-weighed 50-mL [1.7-oz] polycarbonate test tubes. During the transfer process, attempts were made to maximize and evenly distribute the amount of solids placed into the test tubes. Once an adequate amount (based on qualitative observation) of solids had been transferred to each tube, additional solution from the combined test cell mixture was added to bring the total volume of each tube to about 20 mL [0.68 oz]. A total of 10 tubes were filled, weighed to determine the amount of solid and solution added, and separated into 2 groups of 5 for the addition of the neptunium standard solutions. The two groups were labeled NpCSA and NpCSB. Aliquots of the original mixed test cell solution were withdrawn for chemical analysis. The aliquots were centrifuged and passed through 0.45-μm [1.8×10^{-2}-mil] filters. Samples submitted for cation and trace metal analyses were preserved using nitric acid.

Two Np-237 standard solutions, one for each group of five tubes, were used to spike the corrosion product experimental solutions. One standard solution had a Np-237 concentration of ~100 ppm in a dilute HNO_3 matrix with an estimated pH of 2.5. The second standard solution had a neptunium concentration of about 60 ppm and had been adjusted via the addition of NaOH to a pH of about 5.6. Approximately 100 mL [3.38 oz] of the Np-237 standard solutions (the 100 ppm solution to Group A and the 60 ppm solution to Group B) were added to each experimental test tube to give an initial Np-237 concentration of 1.8×10^{-6} M for Group A and 1×10^{-6} M for Group B. Following the addition of the Np-237 spike, the experimental test tubes were loosely capped to facilitate gas exchange with the atmosphere and placed on a gyratory shaker.

After 7 days, the experimental solutions were re-weighed, sampled to determine Np-237 concentration, and measured for pH. Prior to removing the aliquots for Np-237 analysis, the experimental test tubes were centrifuged for 10 minutes at 10,000 rpm in a Fisher Marathon 21K centrifuge. Based on the centrifuge rotor dimensions and an assumed density of 3.9 g/cm^3 [1.41×10^{-1} lb/in^3] (Dzombak and Morel, 1990) for the corrosion products (equivalent to

ferrihydrite or iron oxyhydroxide), particles greater than 0.08 μm [3×10^{-3} mil] in diameter should have been removed from solution by settling. Np-237 concentrations were determined by counting their alpha emissions in a Packard 3100AB/TR Liquid Scintillation Analyzer. Following pH measurement, four solutions in each experimental group were sampled for chemical analyses. Samples were passed through 0.45-μm [1.8×10^{-2}-mil] filters, and samples submitted for cation and trace metal analyses were preserved using nitric acid.

The amount of solid actually added to each experimental test tube was measured by removing as much solution from each tube as possible without disturbing the solid residual and placing the tube and solid in an oven {at 40 °C [104 °F]} to dry. The test tubes and solid residuals contained within were re-weighed after drying, and the carbon steel corrosion product mass in each tube was determined by subtracting the original test tube mass from that of the test tube and dried solid together. Two experimental solutions, one from each group, were held in reserve in case subsequent testing was needed on hydrated samples. The mass of solid in these two tubes was not determined; however, the oxidation-reduction potential of these two solutions was measured using a Ag/AgCl electrode.

4 RESULTS AND DISCUSSION

Information included in this chapter includes the pH and chemical composition evolution of simulated J–13 Well water and simulated sodium-pore water after the immersion of carbon steel and simulated high-level waste glass. In addition to the immersion tests, neptunium-sorption on the corrosion products was examined to assess the capability of carbon steel corrosion products to sorb neptunium.

4.1 Carbon Steel and Glass Immersion Results

4.1.1 Tests in 250-mL [8.45-oz] Glass Cells at 60 °C [140 °F] and 90 °C [194 °F]

Figure 4-1 plots the pH evolution of two tests conducted at 60 °C [140 °F] and 90 °C [194 °F] in simulated J–13 Well water. For these two tests, the test cells were not lined with polytetrafluoroethylene. The water was in direct contact with the glass cell. After the carbon steel specimens were immersed in solution, the pH rose from about 8.3 at the start of the test to about 9.2 in 5 days. For the test at 60 °C [140 °F], the pH continued to increase until it reached 9.6 after 23 days and remained between 9.5 and 9.8 during the remaining test duration. For the test at 90 °C [194 °F], after the initial pH increase to about 9.1, the pH decreased to 8.8 and it remained relatively constant.

For the test at 60 °C [140 °F], a total of 13-mL [0.44-oz] solution was drawn for iron, silicon, and sulfur content analysis, and for the test at 90 °C [194 °F] a total of 11-mL [0.37-oz] solution was drawn. No fresh solution was added to compensate for solution loss. Table 4-1 summarizes the chemical composition analysis results. No detectable iron was present in the liquid phase samples. This suggests that corroded carbon steel precipitates rather than forming soluble phases in solution. Figure 4-2(a) plots the silicon content from these two tests, which increased continuously with time and was higher for the test at 90 °C [194 °F] than at 60 °C [140 °F]. The silicon in solution is attributed to glass dissolution from test cells or silicon leaching from carbon steel specimens at elevated temperatures. The higher silicon content at 90 °C [194 °F] indicates that the glass dissolution rate increased with increasing temperature. The pH increase observed in Figure 4-1 could be partly due to glass dissolution. Figure 4-2(a) shows that at 60 °C [140 °F], the sulfur content remained constant, whereas it increased with time at 90 °C [194 °F].

Tests and post-test visual examination revealed grey to black carbon steel corrosion products precipitated at the bottom of the test cell. Based on the weight change of carbon steel specimens and using the density of carbon steel of 7.87 g/cm^3 [0.284 lb/in^3], the corrosion rates were calculated to be 11.1 and 4.44 × 10^{-3} µm/yr [0.433 and 1.75 × 10^{-4} mil/yr], respectively, at 60 °C [140 °F] and 90 °C [194 °F]—lower than the rates used by the U.S. Department of Energy (DOE) in the in-package chemistry model {72 µm/yr [2.8 mil/yr]} (Bechtel SAIC Company, LLC, 2004a). Figure 4-2(b) shows the optical and scanning electron microscopy photographs of the corroded carbon steel specimens. Less corrosion was observed from the test at 90 °C [194 °F], which is consistent with the observed lower corrosion rate. Scanning electron microscopy photographs show the presence of several mineral phases on the carbon steel surface at 60 °C [140 °F], whereas there was one mineral phase present on the surface at 90 °C [194 °F]. Further analysis of phase composition was not performed.

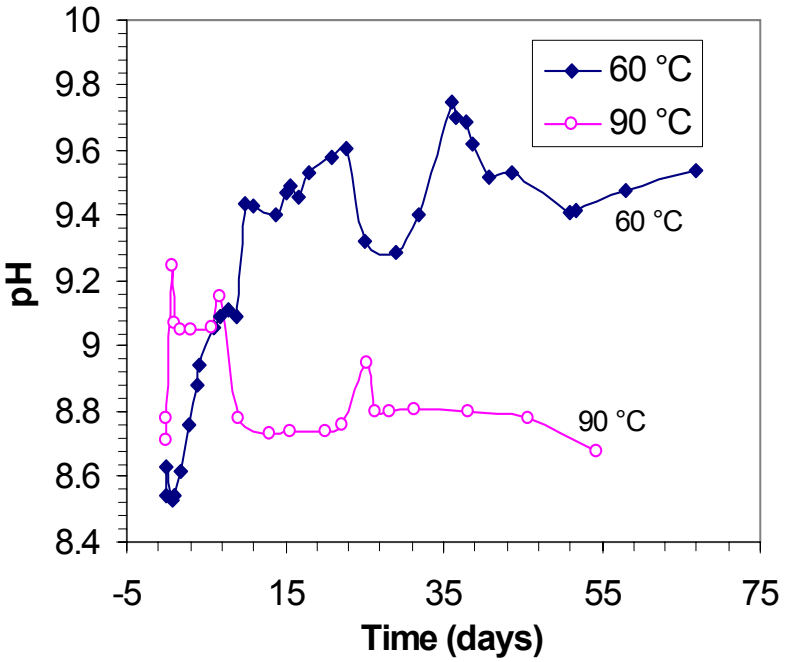

Figure 4-1. pH Evolution of Simulated J–13 Well Water After the Immersion of A516 Carbon Steel Specimens at 60 °C [140 °F] and 90 °C [194 °F]. The Ratio of Water Volume-to-Surface Area of Carbon Steel Was 13.7 mL/cm^2 [2.99 oz/in^2]. The Tests Were Performed in 250-ml [8.45-oz] Glass Test Cells Equipped with Water-Cooled Condenser.

4.1.2 Tests in 60-mL [2.0-oz] Polytetrafluoroethylene Vessel at 60 °C [140 °F]

To avoid glass dissolution from glass test cells, two tests were performed in polytetrafluoroethylene vessels at 60 °C [140 °F]. The starting solution used was simulated J–13 Well water, but the pH was adjusted to about 7 with perchloric acid. The vessel was kept in an oven preset at 60 °C [140 °F]. For one test, about a 1-mm [40-mil] diameter hole was drilled in the lid to allow the solution to equilibrate with air. For the other test, the cell lid was tightly closed. Occasionally, the lid was opened to air to measure pH and draw solution for chemical composition analysis.

Figure 4-3 plots the pH evolution of these two tests. After carbon steel was immersed in solution, the pH increased from 7 to about 9. The open test was terminated in 20 days because two-thirds of the solution evaporated during the testing period. For the test performed in a closed vessel, two simulated SRS–202G high-level waste glass discs with a combined surface area of 4 cm^2 [0.6 in^2] were added to the test cell at 28 days. The surface area ratio of carbon steel-to-glass was 0.9. After the addition of the glass sample, the pH continued to rise to about 10. For this test, a total of 18-mL [0.61-oz] solution was drawn for iron, silicon, sulfur, and boron analysis. Table 4-2 summarizes the analysis results. In aqueous phase, the iron content was below the detection limit. Before the addition of glass, the silicon concentration was below the detection limit, which suggests that the silicon content increase in the aqueous phase from

Table 4-1. Iron, Silicon, and Sulfur Concentration in Simulated J–13 Well Water After the Immersion of Carbon Steel Specimens at 60 °C [140 °F] and 90 °C [194 °F]							
60 °C [140 °F]				90 °C [194 °F]			
Time (days)	Iron (mg/L*)	Silicon (mg/L*)	Sulfur (mg/L*)	Time (days)	Iron (mg/L*)	Silicon (mg/L*)	Sulfur (mg/L*)
0.097	<2.50	3.32	N/D†	0.021	<2.50	6.82	N/D†
1.0	<2.50	5.40	N/D†	0.067	<2.50	26.5	N/D†
2.7	12.2‡	7.40	N/D†	1.7	<2.50	36.5	N/D†
3.8	6.82‡	7.96	N/D†	3.0	<2.50	42.9	N/D†
6.8	8.91‡	11.2	N/D†	5.7	<2.50	49.9	N/D†
8.8	16.0‡	13.3	N/D†	13	<2.00	53.8	9.63
14	12.5‡	18.3	N/D†	20	<2.00	54.3	13.2
21	4.86‡	21.7	N/D†	25	<2.00	59.4	15.6
29	2.55‡	22.2	3.86	31	<2.00	60.2	18.4
36	<2.00	24.8	3.29	38	<2.00	62.3	19.2
38	<2.00	26.0	3.21	54	<2.00	82.9	23.2
44	<2.00	29.2	3.29	*1 mg/L = 8.35×10^{-6} lb/gal †N/D = Not determined ‡Solid phase was dissolved and combined with liquid phase for composition analysis using inductive coupled plasma method			
51	3.49	20.0	4.47				
67	<2.00	26.8	4.18				

the glass test cell [Figure 4-2(a)] was mainly due to glass dissolution from the glass cell rather than from silicon in carbon steel specimens. After adding glass, the silicon and boron concentration in solution increased with time; however, the iron and sulfur concentration remained relatively constant.

During the tests, solution with corrosion precipitates was drawn periodically for particle size distribution analysis. Sequential analysis of corrosion products shows no time dependence of particle size distribution. Figure 4-4 shows the analysis results of particles drawn after the carbon steel was immersed for 67 days. Most particles were observed in the micrometer range and no evidence of colloids existed in solution. The test was terminated at 74 days.

Figure 4-5 shows the optical photographs of the carbon steel and high-level waste glass specimens after immersion and x-ray diffraction of the corrosion products on the carbon steel surface from the test in the closed polytetrafluoroethylene vessel. The carbon steel specimen was covered with corrosion deposits and the glass discs were partly covered with carbon steel

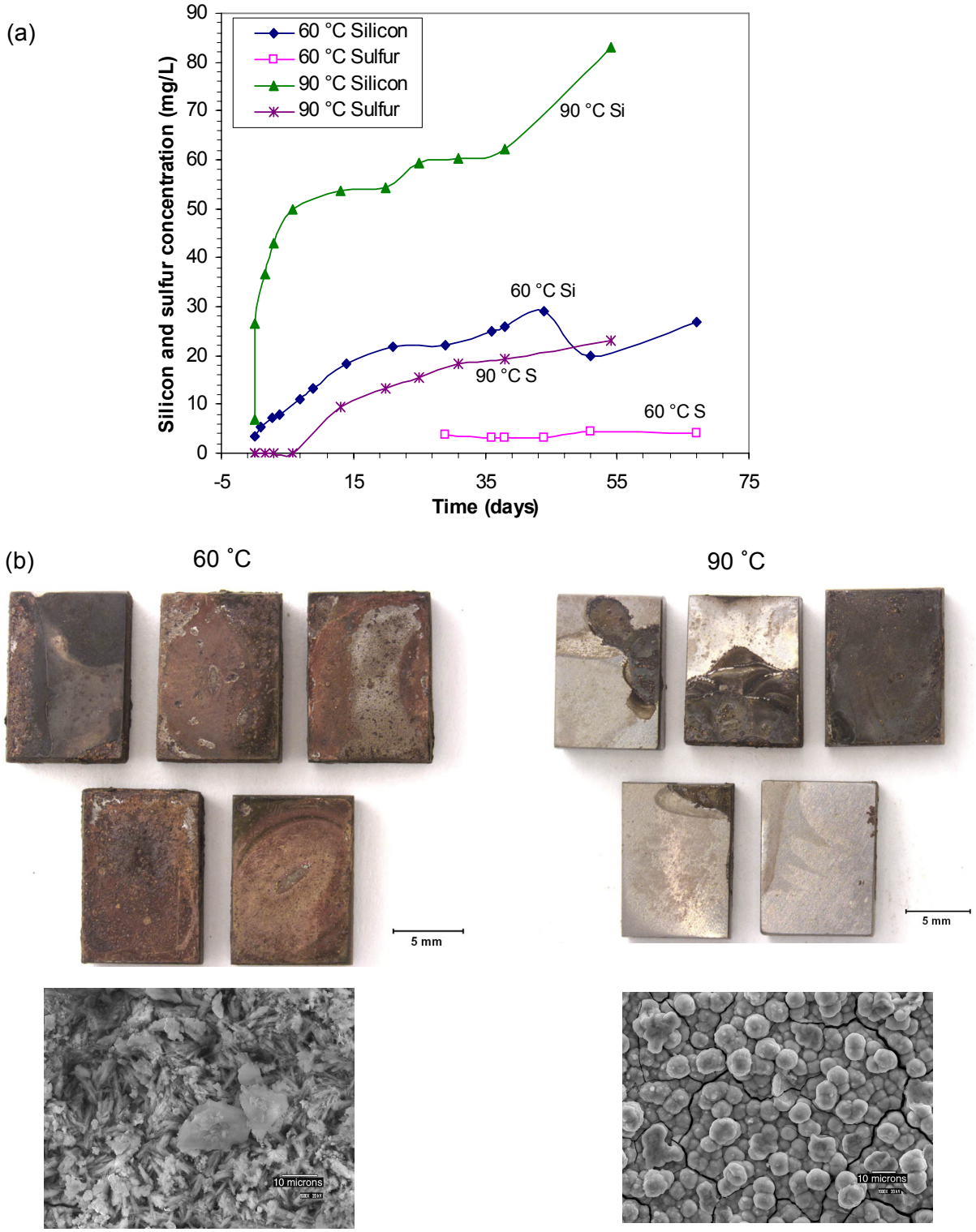

Figure 4-2. (a) Evolution of Silicon and Sulfur Concentration in Simulated J–13 Well Water as Carbon Steel Specimens Were Immersed in 250-mL [8.45-oz] Glass Test Cells at 60 °C [140 °F] and 90 °C [194 °F]. (b) Optical and Scanning Electron Microscope Photographs of Carbon Steel Specimens After Immersion.

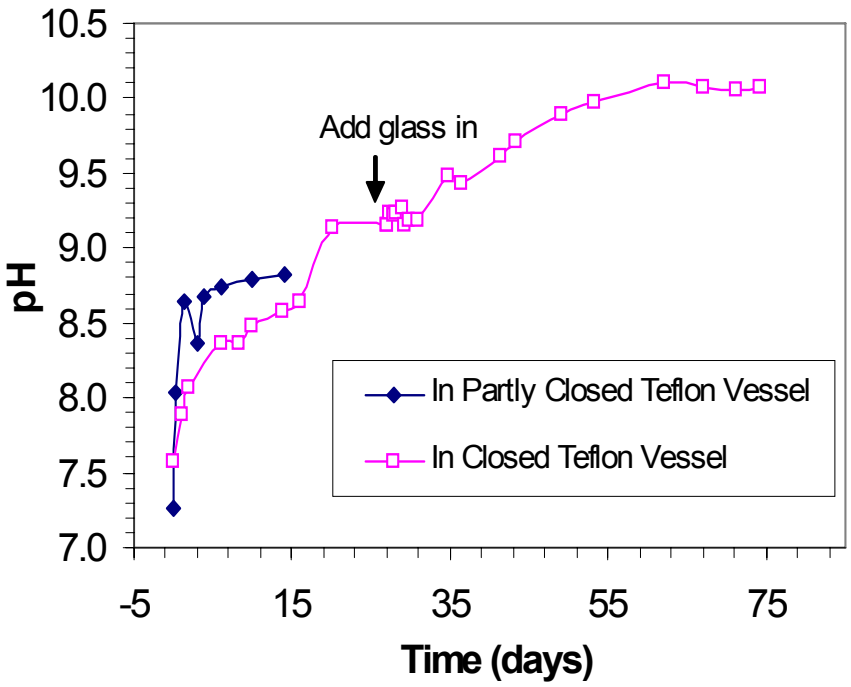

Figure 4-3. pH Evolution of Simulated J–13 Well Water After the Immersion of Carbon Steel Specimens at 60 °C [140 °F]. The Ratio of Solution Volume-To-Surface Area of Carbon Steel was 13.7 mL/cm^2 [2.99 oz/in^2]. The Tests Were Performed in 6-mL [2.0-oz] Polytetrafluoroethylene Vessel with Lid Partly Closed and with Lid Completely Closed, Respectively.

corrosion products. Magnetite (Fe_3O_4) and the matteuccite ($NaHSO_4 \cdot H_2O$) were confirmed by the x-ray diffraction analysis of the corrosion deposits on carbon steel surface. The carbon steel corrosion rate was calculated to be 11.7 µm/yr [0.461 mil/yr] from the weight loss measurements. Figure 4-6 shows the scanning electron microscopy photographs and energy dispersion x-ray spectroscopy of the corrosion products precipitated in the solution. The corrosion products consisted of several mineral phases with different shapes and were primarily iron oxides with small amounts of silicon as revealed by energy dispersion x-ray spectroscopy.

4.1.3 Tests in 250-mL [8.45-oz] Glass Test Cells with Polytetrafluoroethylene Liner at 60 ˚C [140 ˚F]

There were four test cells (Cells #1, #2, #3, and #4) running in parallel at the same conditions. The glass test cells were lined with polytetrafluoroethylene liner to minimize direct contact of solution with the glass wall of the test cell. Before the test, about 12 mL [0.41 oz] of deionized water was added into the gap between the glass wall and the liner to assist in heat transport from the outside of the cell to the solution. The starting solution used was simulated sodium-pore water (Table 3-2). The pH of each test cell was monitored using the same pH probe. Solution was periodically drawn from Cell #1 for chemical composition analysis. Once solution was drawn, the same amount of fresh solution was added to compensate for solution

Table 4-2. Evolution of Iron, Silicon, and Sulfur Concentration in Simulated J–13 Well Water After the Immersion of Carbon Steel and Simulated High-Level Waste Glass Specimens at 60 °C [140 °F] in Polytetrafluoroethylene Vessel								
Test in Partly Closed Vessel				**Test in Completely Closed Vessel**				
Time (days)	Iron (mg/L*)	Silicon (mg/L*)	Sulfur (mg/L*)	Time (days)	Iron (mg/L*)	Silicon (mg/L*)	Boron (mg/L*)	Sulfur (mg/L*)
0.031	2.00	<1.00	5.88	0	<1.25	<0.5	<0.25	5.36
0.18	<2.00	<1.00	5.80	0.95	<1.25	<0.5	<0.25	5.73
1.2	<2.00	<1.00	6.05	1.9	<1.25	<0.5	<0.25	5.46
3.0	<2.00	<1.00	6.12	5.9	<1.25	<0.5	<0.25	5.41
4.0	<2.00	<1.00	6.39	10	<1.25	<0.5	<0.25	5.62
6.0	<2.00	<1.00	6.70	16	<1.25	<0.5	<0.25	5.36
10	<2.00	<1.00	7.39	20	<1.25	<0.5	<0.25	5.37
*1 mg/L = 8.35×10^{-6} lb/gal				27	<1.25	<0.5	<0.25	5.38
				Add Simulated SRS-202G High-Level Waste Glass				
				28	<1.25	1.55	0.318	5.22
				29	<1.25	2.94	0.611	5.26
				35	1.04	5.99	2.18	6.30
				36	<1.00	6.64	2.76	5.91
				49	1.37	10.4	5.54	5.30
				53	1.47	11.2	6.34	5.16
				74	5.63	16.8	10.5	4.21

loss. In Cell #4, one carbon steel specimen was connected to a stainless steel rod for corrosion potential monitoring. A Luggin probe was immersed in the solution. Except for the tip, the outside of the Luggin probe was wrapped with polytetrafluoroethylene tape to minimize glass dissolution.

Figure 4-7 plots the pH evolution of these four test cells. After carbon steel specimens were immersed in solution, the pH increased linearly from the starting pH to values in the range of 9.1–9.5 due to carbon steel dissolution. After an initial increase, the pH of all the test cells decreased slightly around 20 days. However, the pH continued to increase with time for Cell #2

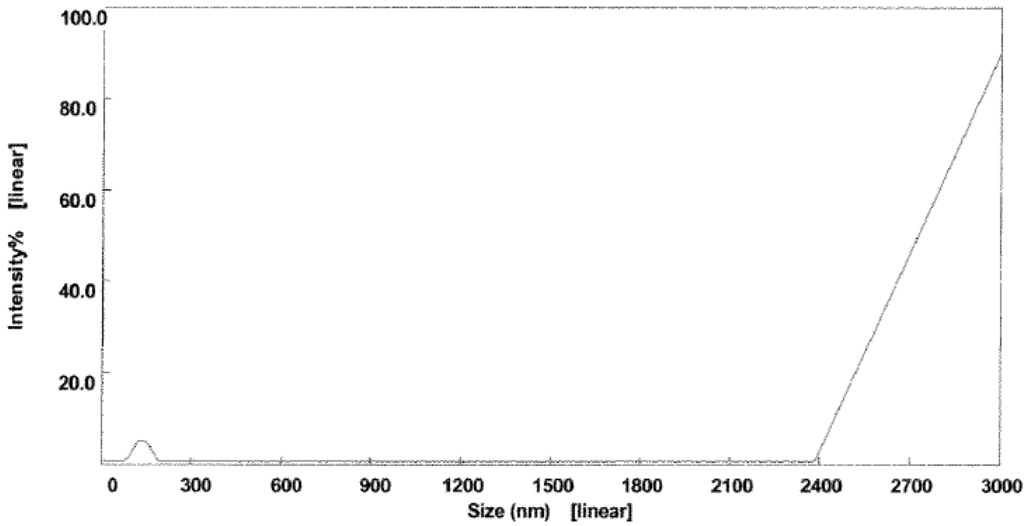

(a) Submicron Particle Size Analysis Using Photon Correlation Spectroscopy

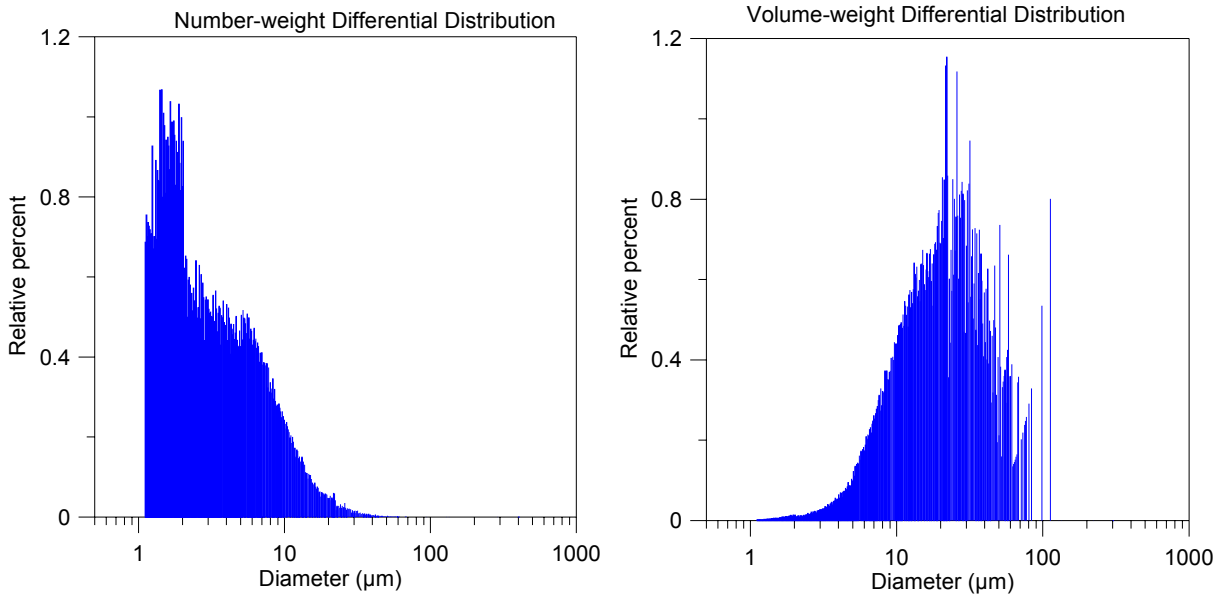

(b) Micron Particle Size Analysis Using Optical Counter

Figure 4-4. Carbon Steel Corrosion Product Size Distribution Analysis after Carbon Steel Was Immersed in Simulated J–13 Well Water at 60 °C [140 °F] for 67 Days, (a) Submicron Particle Size Analysis Using Photon Correlation Spectroscopy, and (b) Micron Particle Size Analysis Using Optical Counter.

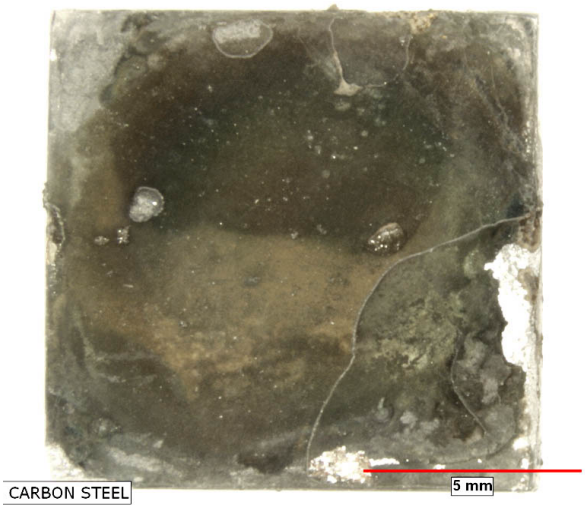

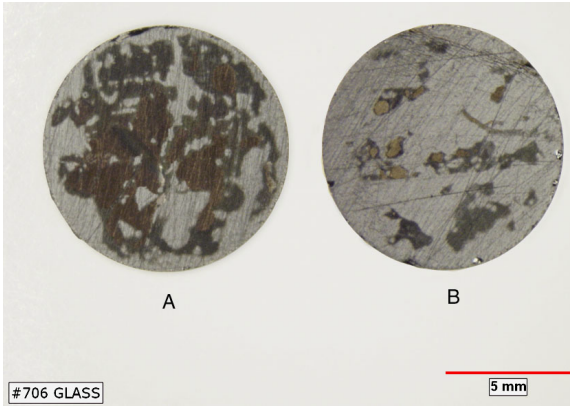

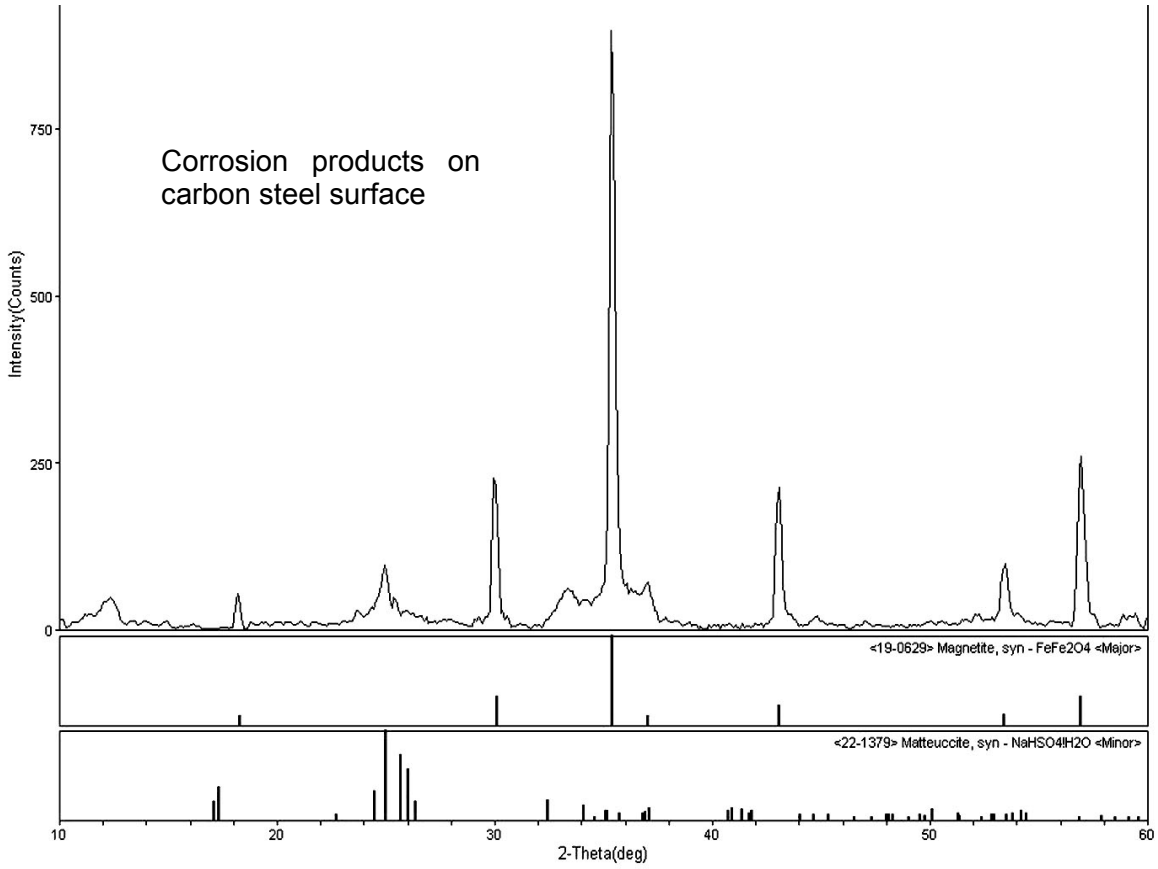

Figure 4-5. Optical Photographs of Carbon Steel and Simulated High-Level Waste Glass Specimen and X-Ray Diffraction of Corrosion Deposits on Carbon Steel After Being Immersed in Simulated J–13 Well Water for 65 Days at 60 °C [140 °F]

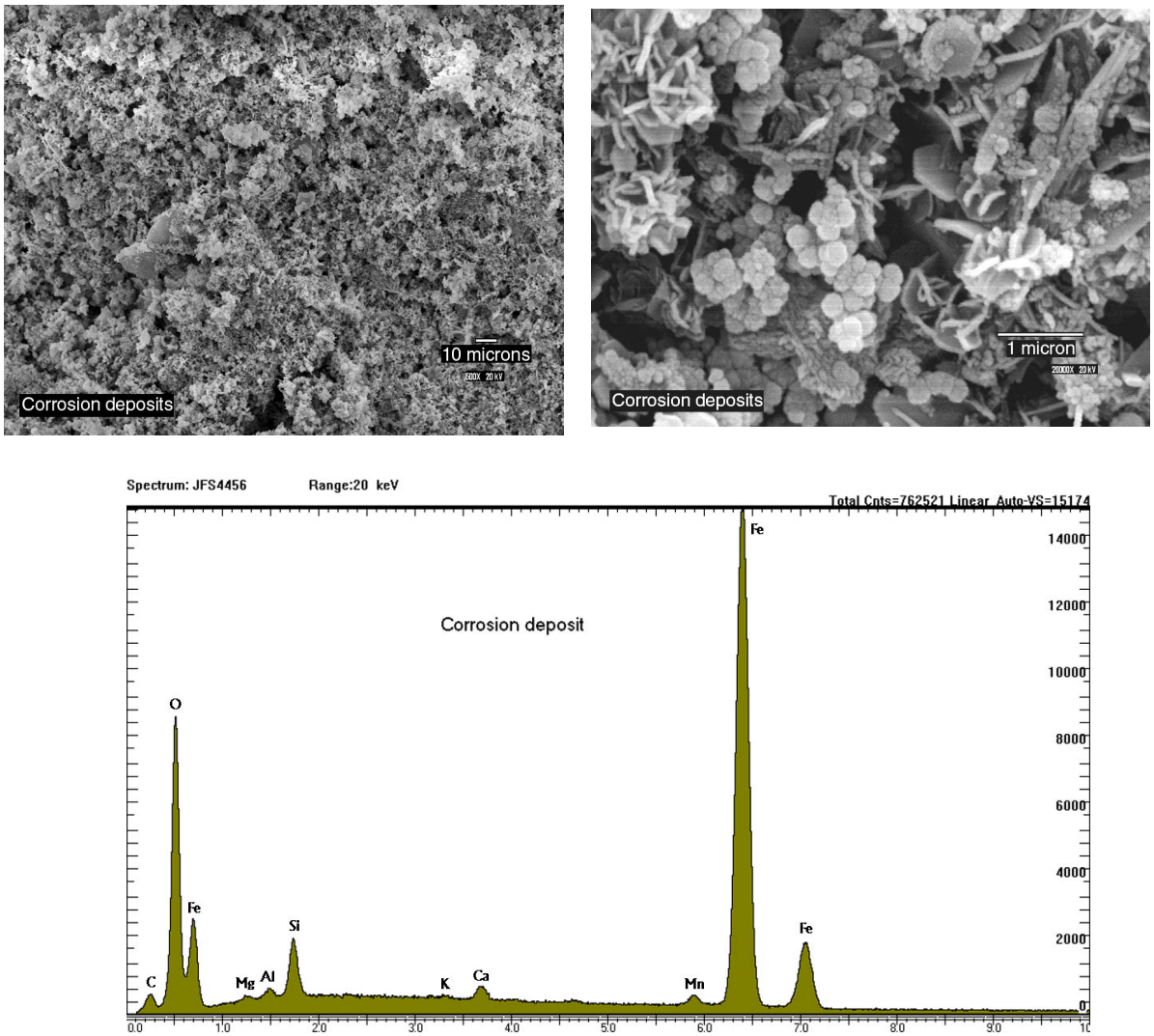

Figure 4-6. Scanning Electron Microscope Photographs of Corrosion Products Precipitated in Solution and Energy Dispersive X-Ray Spectroscopy of the Corrosion Deposits After Carbon Steel and Glass Were Immersed in Simulated J–13 Well Water in Closed Teflon Vessel at 60 °C [140 °F]

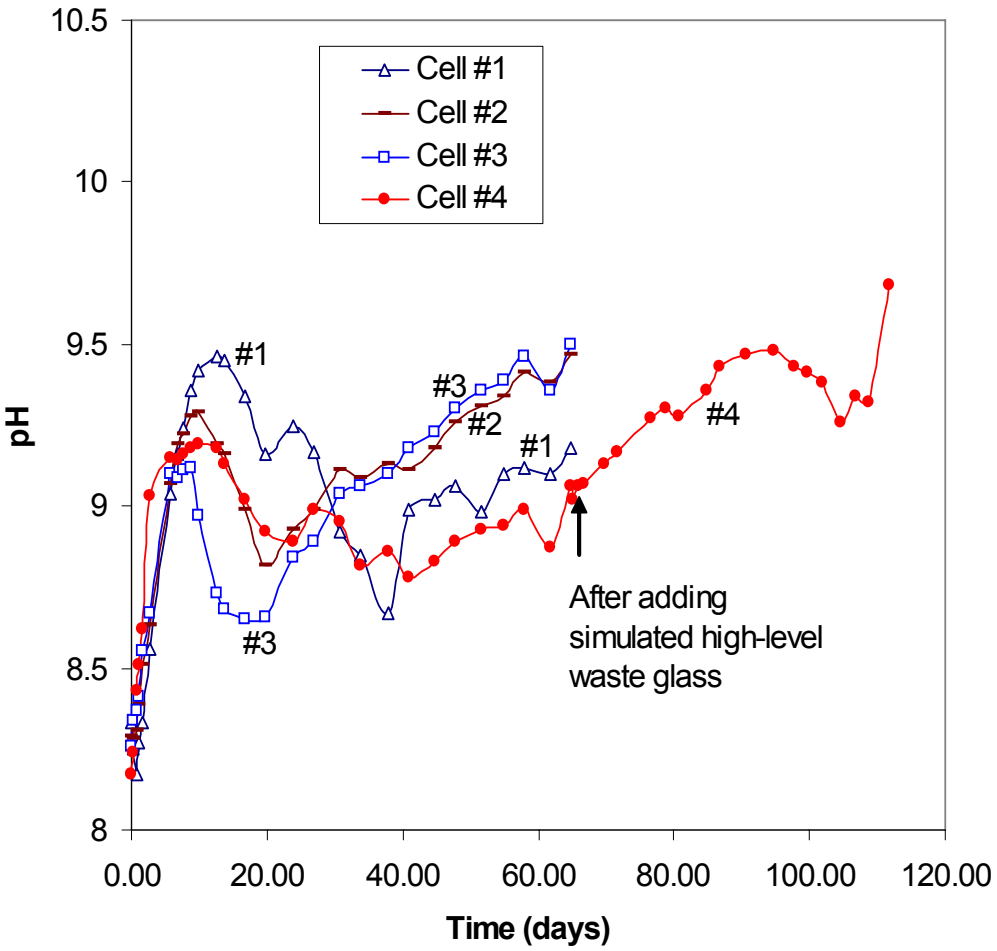

Figure 4-7. pH Evolution of Simulated Pore Water after the Immersion of Carbon Steel with Water Volume to Carbon Steel Surface Area Ratio of 13.7 mL/cm^2 [2.99 oz/in^2] at 60 ˚C [140 ˚F]. Four Test Cells #1, #2, #3, and #4 Were Set Up Under the Same Condition. At 65 Days, Simulated High-Level Waste Glass Was Added Into Cell #4.

and Cell #3 to approximately 9.5, whereas the pH values of Cell #1 and Cell #4 fluctuated between 8.9 and 9.4. Despite the fluctuation, the pH increased by about one unit for all four test cells overall. In Figure 4-7, Cell #1 exhibited similar but delayed behavior to Cells #2 and #3. It was possibly caused by withdrawing samples from Cell #1 for chemical composition analysis and replacing them with fresh solution that disturbed the equilibrium and resulted in delayed behavior. Tests in Cells #1, #2, and #3 were terminated after 65 days. Approximately 1 mL [0.03 oz] of solution was drawn from each test cell for chemical composition analysis and another 1 mL [0.03 oz] of solution with corrosion products was drawn from each test cell for environmental-scanning electron microscopy and particle size distribution analysis. The test solution and corrosion products from these three test cells were combined. The pH of the combined solution at room temperature was 9.72. Most of the solution with the corrosion products was used for radionuclide sorption tests. The remaining corrosion products were

centrifuged and dried in air for phase composition characterization. In test Cell #4, four simulated high-level waste glass disks with total surface area of 8 cm^2 [1.2 in^2] were added into solution after 65 days. The surface area ratio of carbon steel to glass was 4.17. After the addition of glass, the pH continued to increase for Cell #4 as shown in Figure 4-7.

Table 4-3 summarizes the inductive coupled plasma and ion chromatography analysis results for solutions drawn from all test cells along with the calculated concentration of the original simulated sodium-pore water. Figure 4-8 plots ionic concentration evolution with time. Data in Table 4-3 and Figure 4-8 show several notable features

- For all four test cells, the total iron concentration was below the detection limit, consistent with the previously observed results from other tests.

- The calcium concentration decreased with time to ~2 mg/L [2×10^{-5} lb/gal] after 10 days and remained relatively constant afterwards [Figure 4-8(c)], consistent with the predicted speciation calculation using EQ3/6 software.

- The magnesium concentration decreased to below detection limit during the first 20 days [Figure 4-8(d)]. Calcium and magnesium may have precipitated with corrosion products or deposited on carbon steel surface from the energy dispersion x-ray spectroscopy analysis of corrosion products.

- Sodium concentration increased by 50 mg/L [4.2×10^{-4} lb/gal] in 20 days [Figure 4-8(e)]. After the initial decrease, silicon and boron concentrations increased similarly to equilibrium concentrations after about ~30 days [Figure 4-8(f) and (g)]. This could be attributed to glass dissolution.

- Sulfur concentration increased during the first 20 days, but it decreased with time afterwards [Figure 4-8(h)]. This is consistent with the evolution of sulfate concentration [Figure 4-8(m)]. The increase of sulfur could be due to its dissolution from carbon steel, and the decrease could be due to precipitation of sulfate with calcium, magnesium, or other cations.

- Potassium and chloride concentration increased continuously by about 50 mg/L [4.2×10^{-4} lb/gal] and 30 mg/L [2.5×10^{-4} lb/gal], respectively [Figure 4-8(i) and (j)]. This increase could be attributed to KCl leaching from the pH probe while monitoring pH.

- Nitrate concentration increased by about 20 mg/L [1.7×10^{-4} lb/gal] [Figure 4-8(k)]. This could be attributed to dissolution of nitrogen from carbon steel.

- Fluoride concentration remained relatively constant [Figure 4-8(l)], which indicates that the polytetrafluoroethylene liner did not leach out to contribute fluoride into solution.

Table 4-3. pH and Ionic Concentrations in the Simulated Pore Water Drawn From Test Cells with A516 Carbon Steel Immersed at 60 °C [140 °F]

Time (days)	pH	Concentration (mg/L*)										
		Iron	Calcium	Magnesium	Potassium	Sodium	Silicon	Boron	Sulfur	Chloride	Nitrate	Fluoride
Simulated Sodium-Pore Water (Calculated)												
	8.5	0	18.2	3.37	6.2	120	0	0	10.4	24.2	0.42	6.15
Test Cell #1												
1.1	8.3	<1.25	5.05	3.11	<7.50	121	<0.5	<0.5	10.1	N/D‡	N/D‡	N/D‡
2.8	8.6	<1.25	2.33	3.26	<7.50	120	<0.5	<0.5	10.4	N/D‡	N/D‡	N/D‡
5.8	9.0	<1.25	1.30	3.23	11	123	<0.5	<0.5	10.8	N/D‡	N/D‡	N/D‡
13	9.5	<1.25	<1.25	1.59	9.1	131	<0.5	<0.5	11.4	N/D‡	N/D‡	N/D‡
24	9.3	<2.50	1.69	<2.50	21	168	8.35	5.35	14.0	48.5	<1	6.73
34	8.9	<2.50	2.18	<2.50	22	164	7.33	3.65	12.9	45.1	8.6	6.55
52	9.0	N/D‡	N/D‡	N/D‡	N/D‡	N/D‡	N/D‡	N/D‡	11.5	57.6	20.9	6.86
65	9.2	<2.50	1.76	<2.50	65	168	7.28	3.51	11.7	80.2	21.9	6.24
Solution in Gap Between Liner and Glass Cell #1												
65	N/D‡	<2.50	<1.25	<2.50	<5.00	15.6	16.6	5.7	1.03	5.46	13	<1
Test Cell #2												
65	9.5	<2.50	<1.25	<2.50	24	165	7.55	3.95	13.6	49.5	9.5	5.77
Test Cell #3												
65	9.5	<2.50	<1.25	<2.50	34	174	12	4.99	12.4	54	16	5
Test Cell #4												
65	9.1	<2.50	2.38	<2.50	1360	2120	9.09	9.43	18.8	4000	23.4	33.1

*1 mg/L = 8.35×10^{-6} lb/gal
‡N/D = Not determined

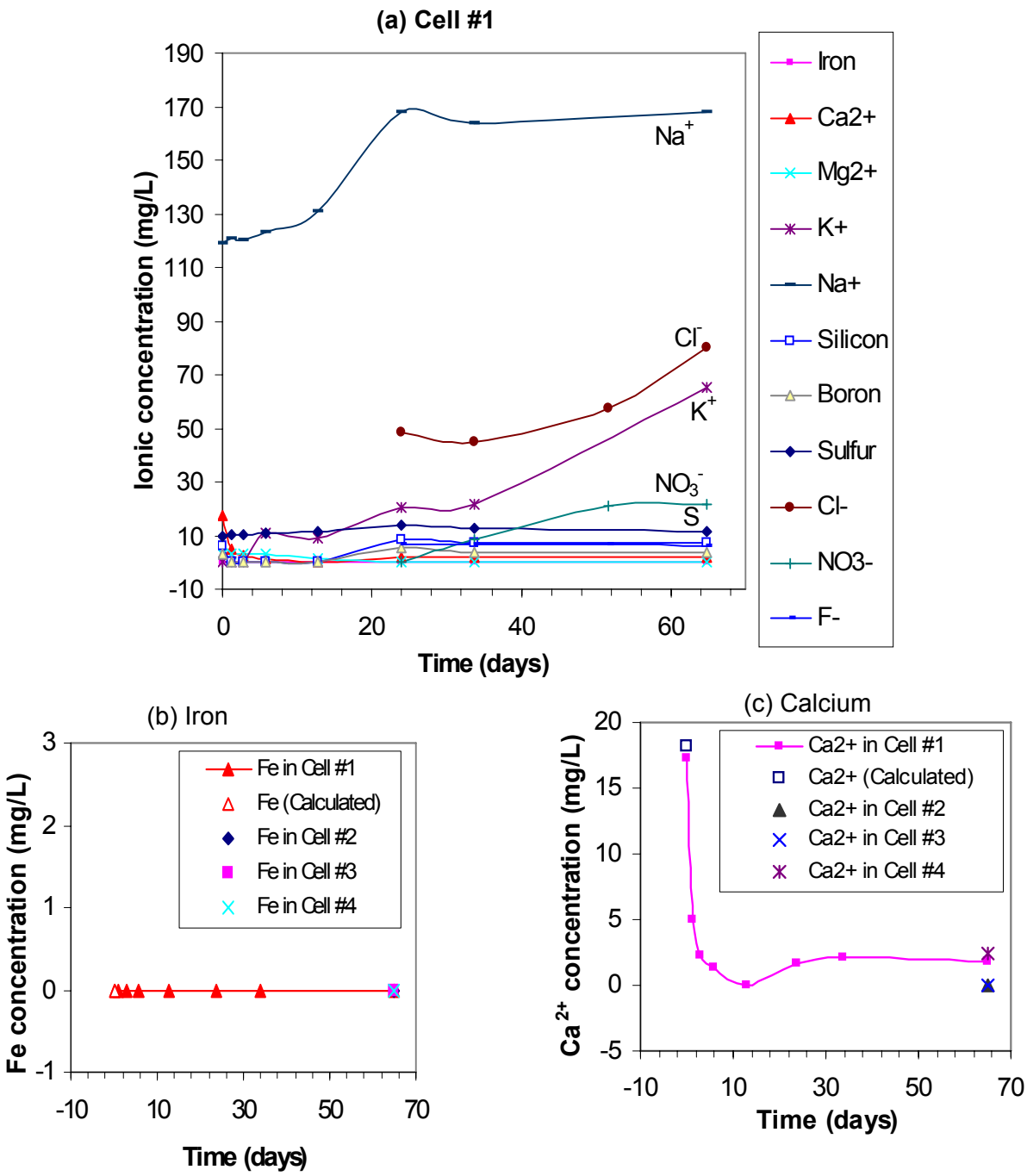

Figure 4-8. Ionic Concentration Evolution of Simulated Sodium-Pore Water in Test Cell #1 After the Immersion of Carbon Steel With Water Volume to Carbon Steel Surface Area Ratio of 13.7 mL/cm^2 [2.99 oz/in^2] at 60 °C [140°F] and Final Concentrations from Test Cells #2, #3, and #4. (a) Evolution of Ionic Concentrations in Test Cell #1, (b) Total Iron Concentration, (c) Calcium Concentration.

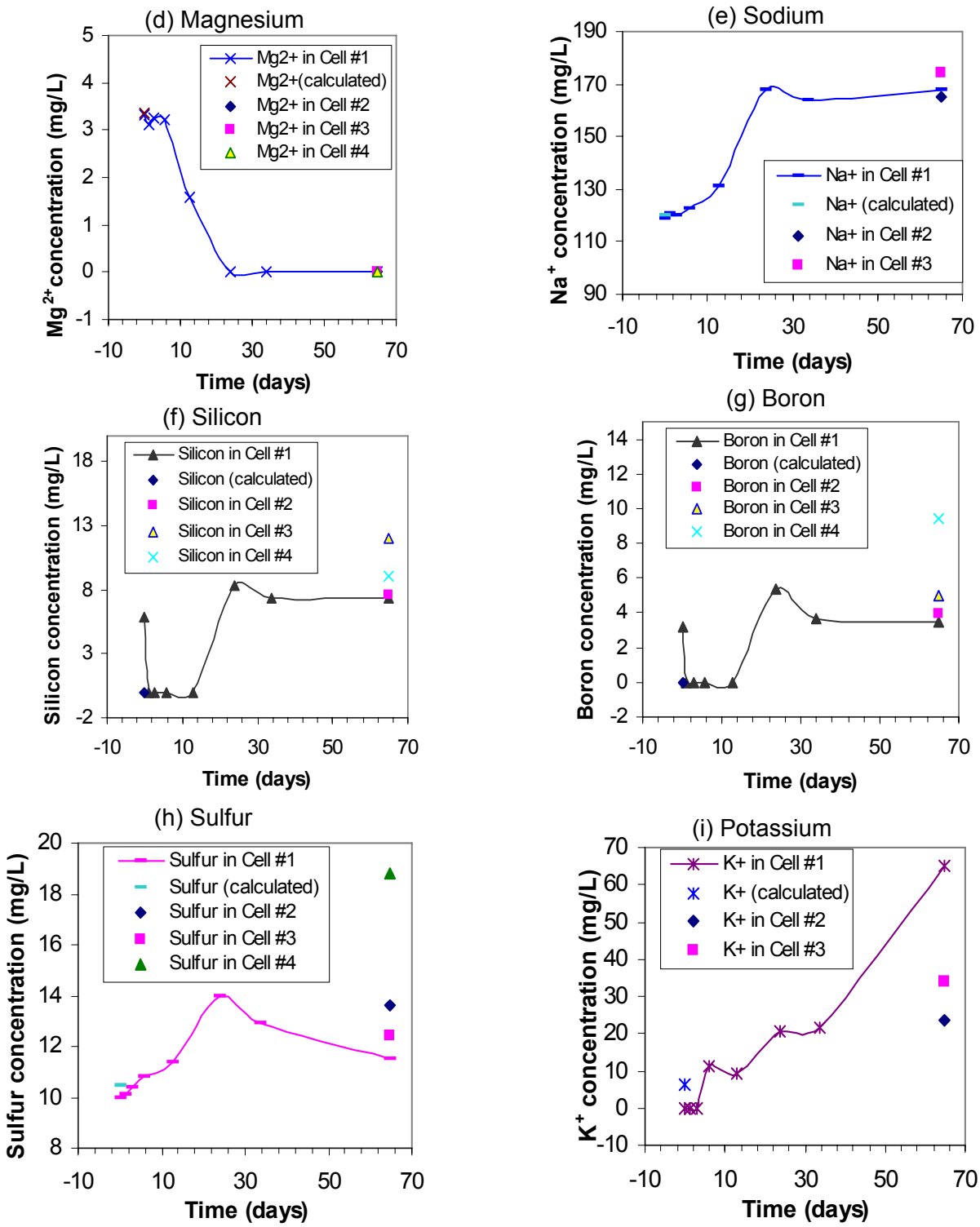

Figure 4-8. (Continued) (d) Magnesium Concentration, (e) Sodium Concentration, (f) Silicon Concentration, (g) Boron Concentration, (h) Sulfur Concentration, (i) Potassium Concentration

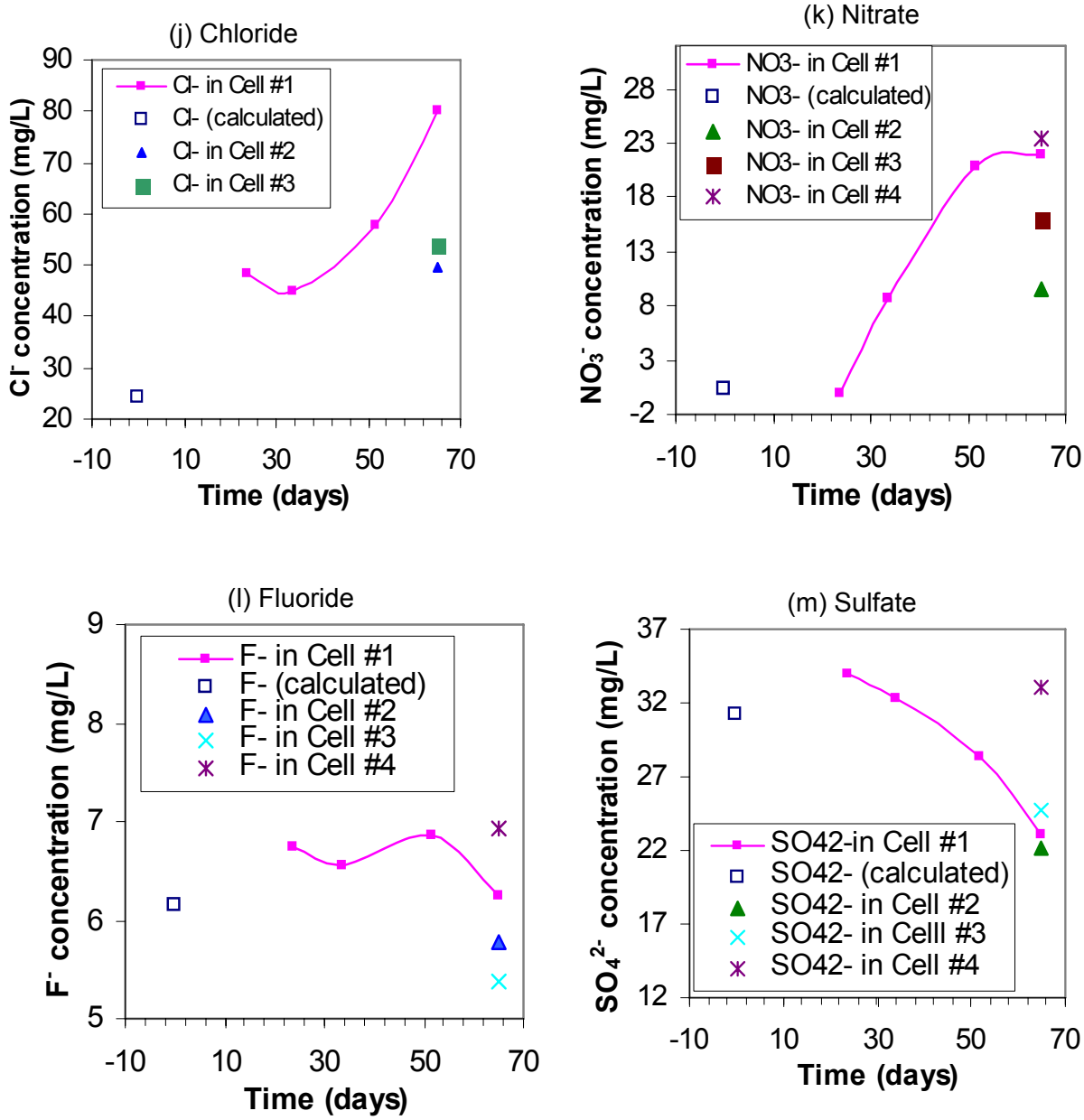

Figure 4-8. (Continued) (j) Chloride Concentration, (k) Nitrate Concentration, (l) Fluoride Concentration, and (m) Sulfate Concentration

Solution was also drawn from the gap between the polytetrafluoroethylene liner and glass for chemical composition analysis. The composition is included in Table 4-3 and was compared to the original solution. Boron, silicon, and sodium concentration increased, which are typical features of glass dissolution. There was also a small amount of chloride and nitrate present in solution. Chloride could come from condensation of the test solution and nitrate could be due to glass dissolution.

Solutions drawn from Cell #2, Cell #3, and Cell #4 showed similar features as observed from Cell #1. Calcium and magnesium concentration decreased, but boron, sodium, silicon, potassium, chloride, and nitrate concentration increased. Fluoride and sulphate concentration remained relatively constant. Typical features of the chemical composition of the solution drawn from Cell #4 were that the potassium, sodium, and chloride concentration increased by more than 100 times. The potassium and chloride concentration increase could be due to concentrated solution leaching out from the Luggin probe for corrosion potential measurement. Increase in sodium could be due to glass dissolution.

Figure 4-9(a) shows particle size distribution analysis results for corrosion products drawn from Cell #1. In the micrometer range, most particles ranged from 0.5 to 3 μm [0.02 to 0.1 mil]; however, a small number of large particles in solution contributed significant weight and volume. Analysis in the nanometer range showed no particles. Environmental-scanning electron microscope photographs of particles in solution in Figure 4-9(b) showed that the particles primarily consisted of well-crystallized cubes, in some places, surrounded by gel-like precipitates. *Ex-situ* Raman spectroscopy and x-ray diffraction were used for *ex-situ* identification of the phases in corrosion products. The results are shown in Figure 4-10. The air-dried corrosion products only showed two broad Raman peaks [Figure 4-10(a)]. The stronger peak at 550 to 800 cm^{-1} [1,397 to 2,032 in^{-1}] could be associated with magnetite (Fe_3O_4), and the peak at 1,300 to 1,400 cm^{-1} [3,302 to 3,556 in^{-1}] could be associated with α-FeOOH, β-FeOOH, or γ-FeOOH. Further *ex-situ* and *in-situ* analyses are needed to identify these peaks. X-ray diffraction of the air-dried corrosion products in Figure 4-10(b) shows that the main mineral phase was magnetite (Fe_3O_4) with minor amounts of lepidocrocite (γ-FeOOH) and goethite (α-FeOOH).

In-situ visual examination of the corroded carbon steel specimens shows that the surface was covered with black deposits. Figure 4-11 shows the *ex-situ* optical and scanning electron microscopy photographs of the corroded carbon steel specimens. The surface was covered with reddish to black corrosion products consisting of crystalline cubes and plates revealed by scanning electron microscopy photographs. Energy dispersion x-ray spectroscopy of these surface crystals revealed that in addition to iron, there were small amount of magnesium, calcium, silicon, and manganese deposited with the corrosion products. Magnesium, calcium, and silicon must be precipitated from test solution. This could account for the concentration decrease of calcium and magnesium in solution [Figure 4-8(c) and (d)]. X-ray diffraction analysis of the corrosion products on the carbon steel surface (Figure 4-12) revealed that the main phase was magnetite and the minor phase was siderite ($FeCO_3$). The corrosion rate of the carbon steel in simulated sodium-pore water from test Cells #1, #2, and #3 was calculated to be 12.7 ± 1.35 μm/yr [0.500 ± 0.053 mil/yr], which was close to that of tests in simulated J–13 Well water and was lower than what DOE used in model calculation (Bechtel SAIC Company, LLC, 2004a).

Figure 4-13 plots the corrosion potential of carbon steel monitored from Cell #4. After the initial increase of corrosion potential from −700 mV_{SCE} to −450 mV_{SCE}, it stabilized around −500 mV_{SCE}.

(a) Corrosion Product Size Distribution Analysis in Micron Range

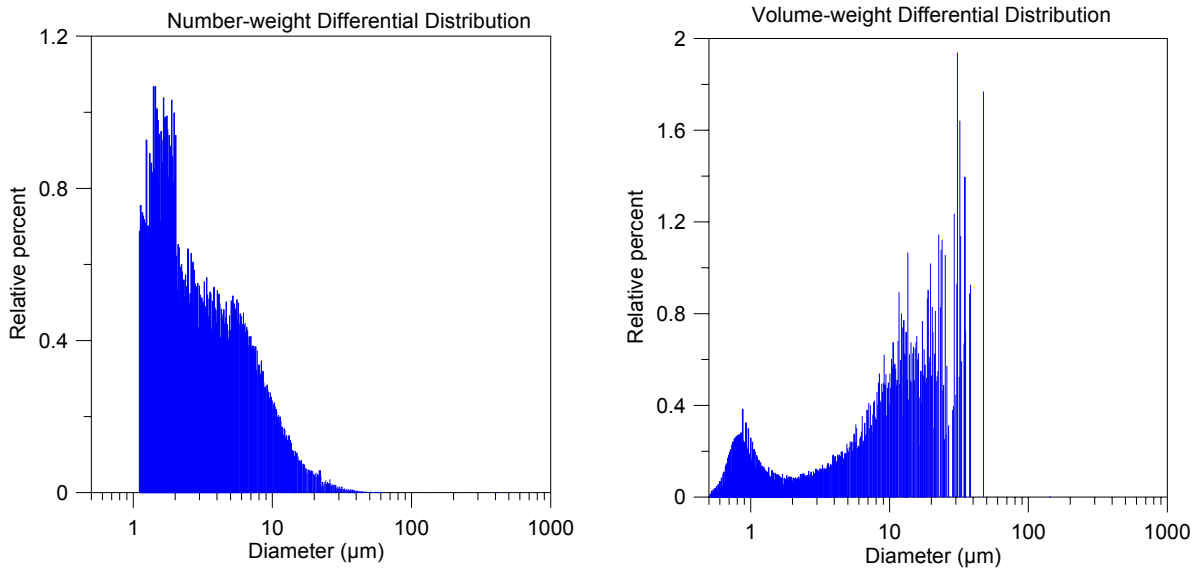

(b) Environmental-Scanning Electron Microscope Photographs of Corrosion Products

Cell #1 Cell #2 Cell #3

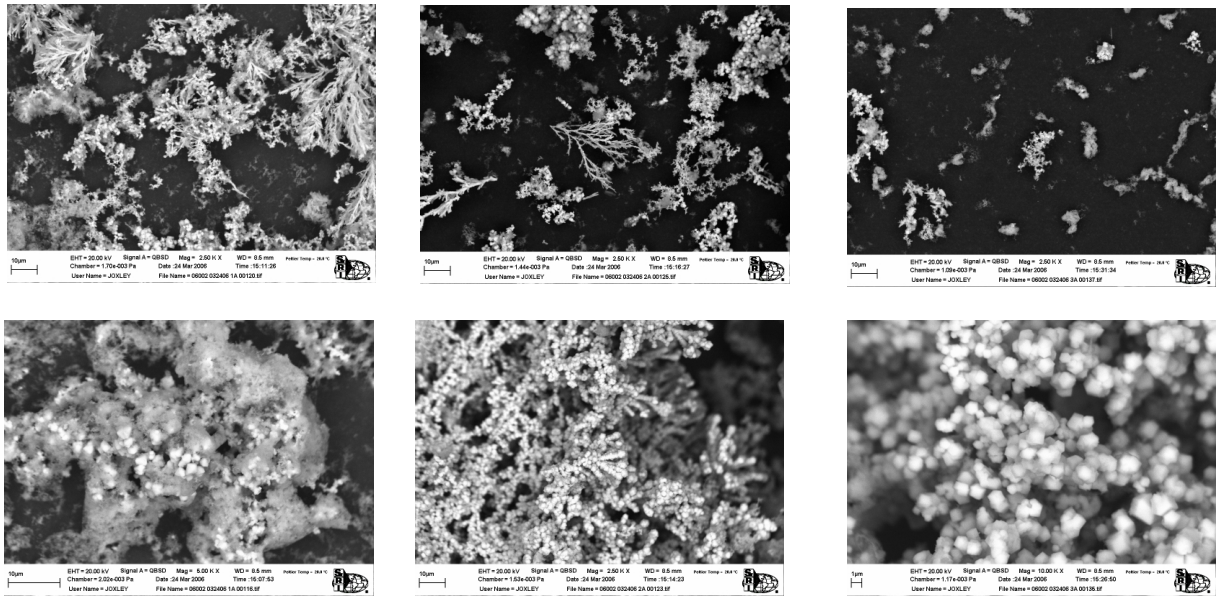

Figure 4-9. (a) Carbon Steel Corrosion Product Size Distribution Analysis from Cell #1 after Carbon Steel Was Immersed in Simulated Sodium-Pore Water at 60 °C [140 °F] and (b) Environmental-Scanning Electron Microscope Photographs of Corrosion Products Obtained from Test Cells #1, #2, and #3

(a) Raman Spectrum

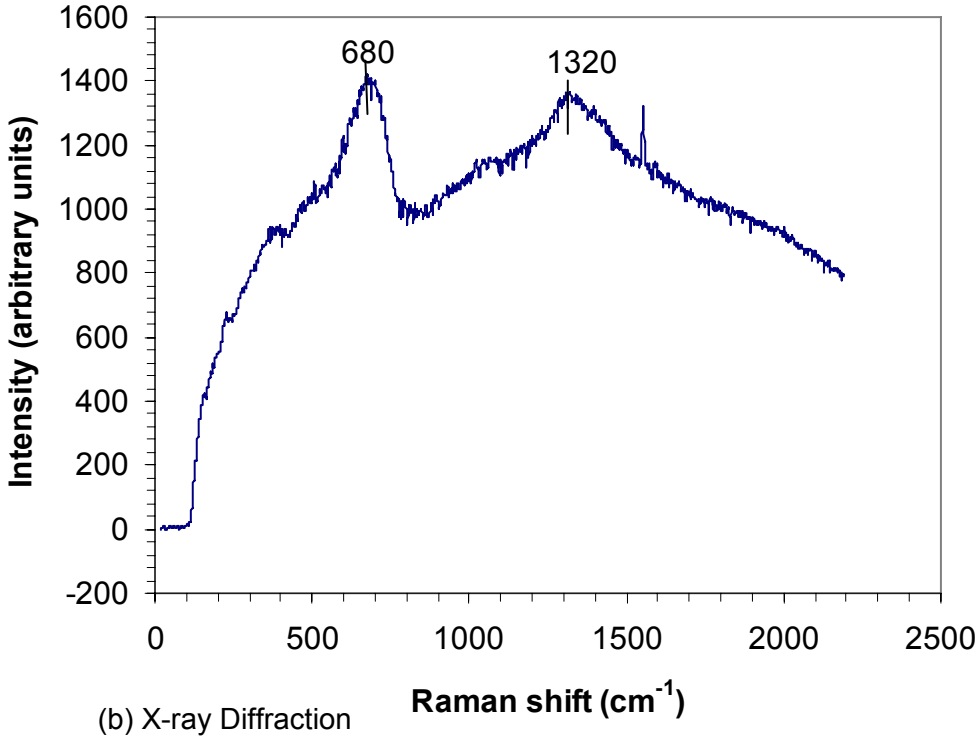

(b) X-ray Diffraction

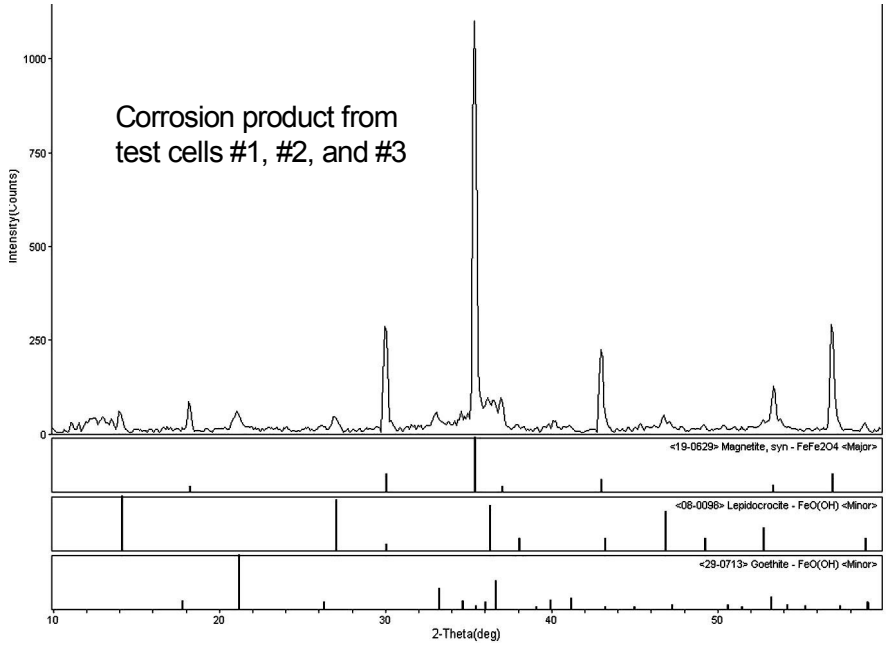

Figure 4-10. (a) *Ex-Situ* Raman Spectrum of Carbon Steel Corrosion Products Collected from Test Cells #1, #2, and #3. The Corrosion Products Were Dried in Air. (b) X-ray Diffraction Spectroscopy of the Same Corrosion Products in (a).

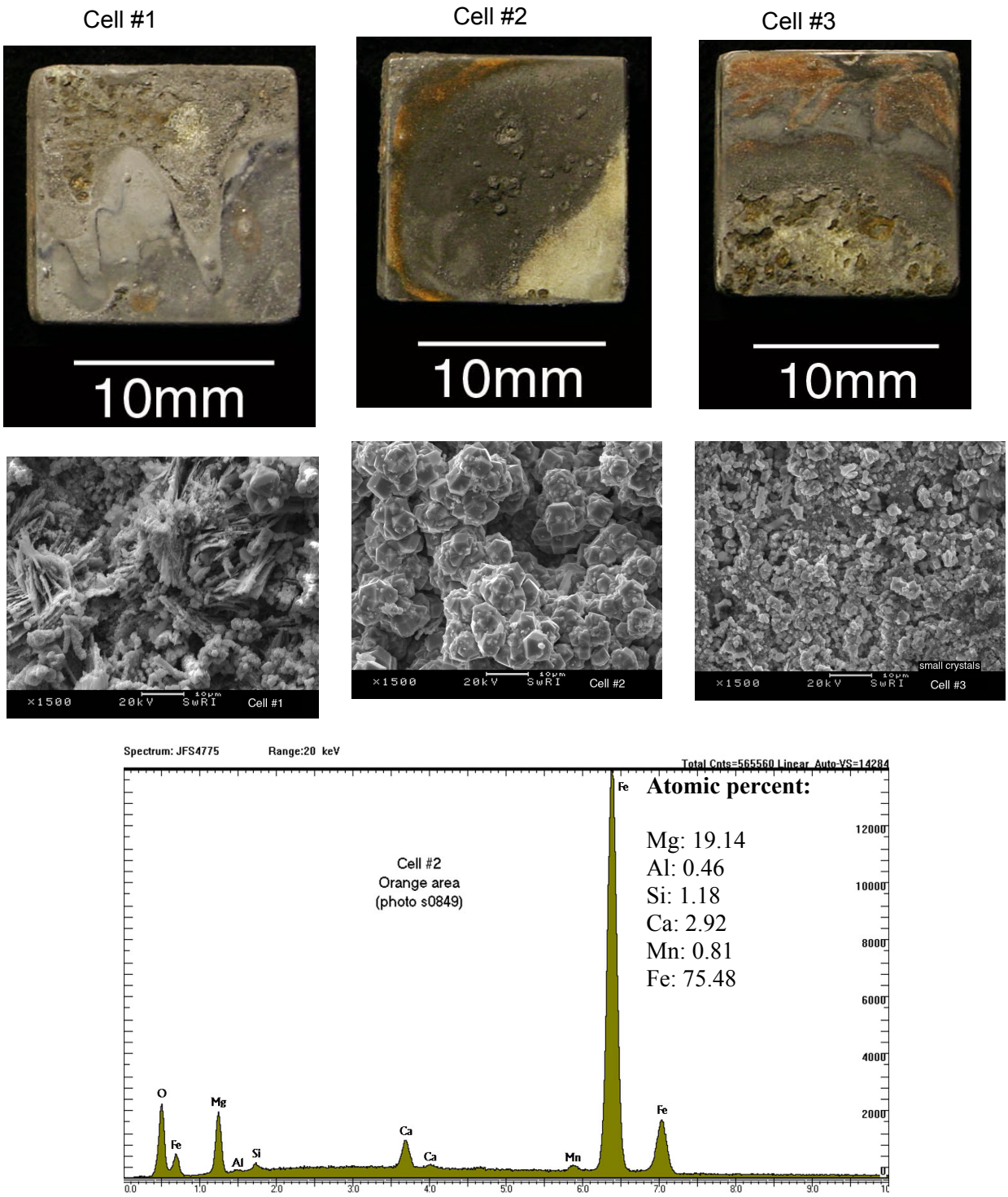

Figure 4-11. Optical and Scanning Electron Microscope Photographs and Energy Dispersive X-Ray Spectroscopy of One Out of Three Carbon Steel Specimens from Each Test Cell After Being Immersed in Simulated Sodium-Pore Water for 65 days at 60 °C [140 °F]

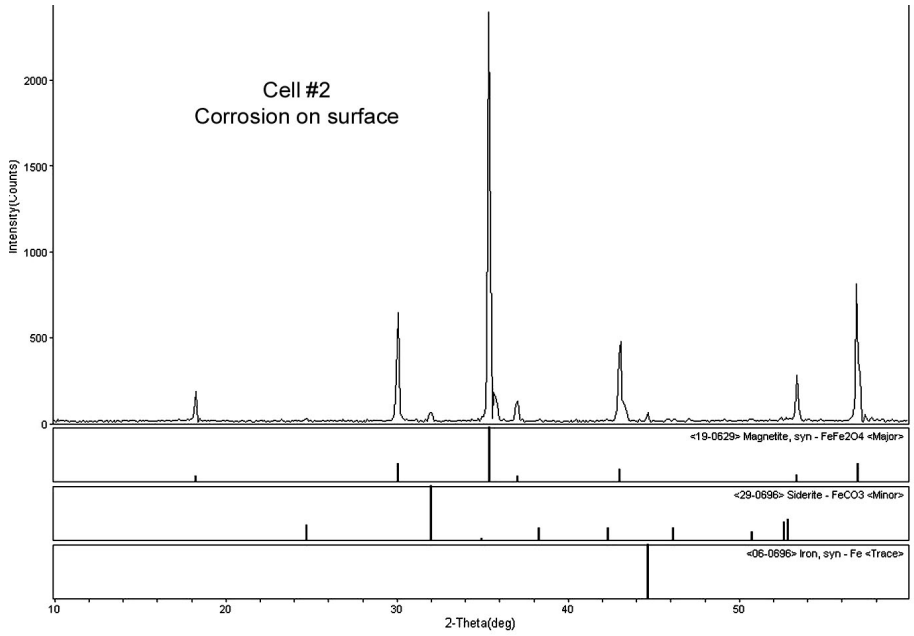

Figure 4-12. Representative X-Ray Diffraction of Corrosion Products on Carbon Steel Surface After Being Immersed in Simulated Pore Water for 65 Days From Test Cell #2 at 60 °C [140 °F]

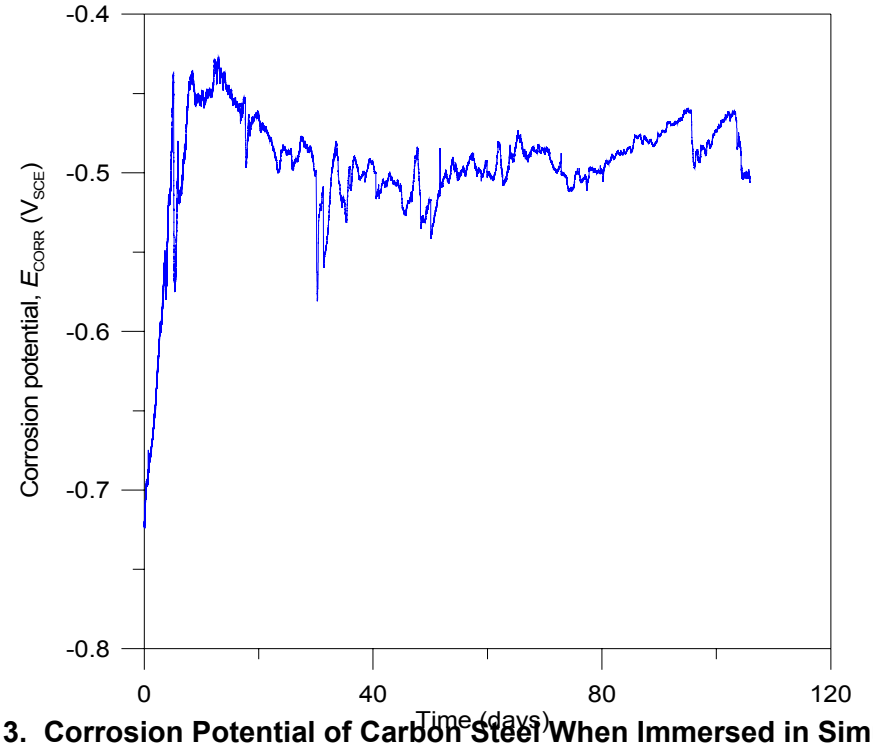

Figure 4-13. Corrosion Potential of Carbon Steel When Immersed in Simulated Pore Water at 60 °C [140 °F] in Test Cell #4

This is about 200 mV higher than the corrosion potential for steel in seawater at room temperature (ASM International, 1987). This potential suggests that the predominant form of iron under such test conditions is $Fe(OH)_2$ and $Fe(OH)_3$ according to the Pourbaix diagram (Pourbaix, 1996). This is consistent with the x-ray diffraction analyses of the corrosion products shown in Figures 4-10 and 4-12.

4.2 Neptunium Sorption Results

The magnitude of sorption of an element or species onto a given substrate is often expressed in terms of a distribution coefficient or K_D. For these experiments, the K_D is the ratio of the concentration of neptunium on the corrosion products to the concentration of neptunium remaining in solution and is expressed by the following equation

$$K_D = \frac{mass\ of\ Np\ on\ solid}{mass\ of\ Np\ in\ solution} \times \frac{V}{m} \tag{4-1}$$

where V is the experimental solution volume and m is the mass of the corrosion product. A summary of the sorption results is plotted in Figure 4-14. The Np-237 K_D values for the carbon steel corrosion products range from 350 to 790 mL/g [5.37×10^{-3} to 1.21×10^{-4} oz/lb]. Experimental Group A, whose solutions generally have lower equilibrium pH values, has an average Np-237 K_D of 514 mL/g [7.88×10^{-3} oz/lb] while Group B has an average Np-237 K_D of 650 mL/g [9.97×10^{-3} oz/lb]. It is apparent that the measured K_D values for each experimental group are not statistically different from each other because there is substantial overlap between the values. The magnitude of neptunium sorption on the corrosion product is substantial {for comparison, montmorillonite clay has a measured K_D for neptunium of about 40 mL/g [6.1×10^{-2} oz/lb] at similar pH values} and is somewhat expected for iron oxyhydroxides (Bechtel SAIC Company, LLC, 2004c; Dzombak and Morel, 1990).

An analysis of the mixed test cell solution and the experimental solution chemistries, however, suggests that it may be difficult to definitively attribute the measured Np-237 K_D values solely to sorption on the iron-based corrosion products. Table 4-4 provides a summary of chemical analyses results for the experimental solutions and the initial mixed test cell solution. The low calcium concentrations for the mixed test cell solution and the experimental solutions relative to the initial simulated pore water prepared for the corrosion test cells indicate a loss of calcium. The calcium concentration dropped from 17.3 mg/L [1.44×10^{-4} lb/gal] in the simulated sodium-pore water (Table 3-2) to between 1 and 2 mg/L [8.35×10^{-6} to 1.67×10^{-5} lb/gal] for the mixed test cell and experimental solutions. Geochemical modeling using the EQ3/6 Version 7.2b code (Wolery, 1992) indicates that calcite is supersaturated in the solutions, and the loss of calcium and magnesium from solution shown in Figure 4.8(c) and (d) is consistent with the precipitation of calcite. The presence of calcite in the corrosion products is a complicating factor, because calcite has been shown to be an effective sorber of neptunium and is particularly effective at removing neptunium from solution by means of co-precipitation or entrainment of neptunium in the calcite structure (Nugent and Turner, 2000; Bertetti, 2002). Figure 4-15 provides a comparison of measured Np-237 K_D values for calcite-bearing alluvium at similar pH values. These high K_D values for the alluvium samples are interpreted to have been caused by neptunium co-precipitation with calcite (Bertetti and Werling, 2005). Figure 4-15 also indicates the range of K_D values used by DOE for sorption of neptunium onto iron oxides (Bechtel SAIC Company, LLC, 2004c). The DOE K_D range and the ranges for

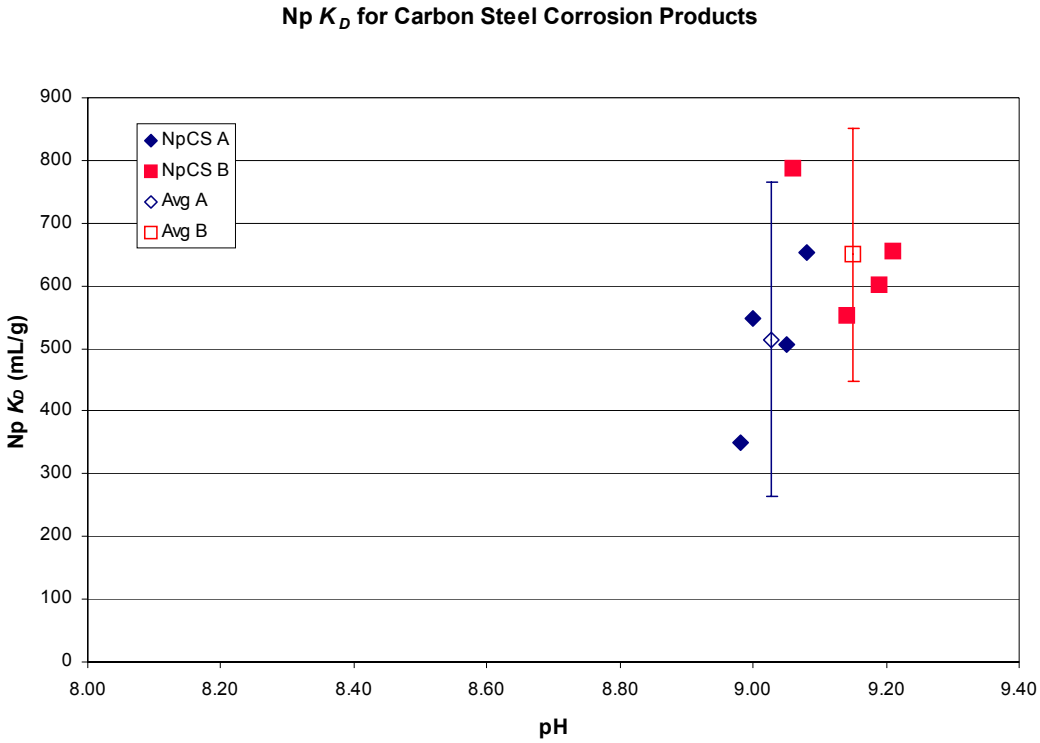

Figure 4-14. Plot of Measured Np-237 K_D Values for the Carbon Steel Corrosion Products from Test Cells #1, #2, and #3. The Open Symbols Indicate Average Values for Each Experimental Group, While the Error Bars Indicate the Two Standard Deviation Ranges for Each Group.

calcite-bearing alluvium and the corrosion products (with calcite) in this study overlap substantially. Thus, the potential presence of calcite within the corrosion products makes it difficult to attribute the sorption of neptunium to the corrosion products rather than to the calcite. Measured oxidation-reduction potentials for solutions NpCSA5 and NpCSB5 were 598 and 588 mV (Eh, hydrogen electrode), respectively, which indicate an oxidizing environment. This suggests that the high K_D values are not a result of reducing conditions within the experiment test tubes.

To verify the presence of calcite in the corrosion products as predicted by geochemical modeling, a simple acid test was conducted on dried corrosion product material from two of the experimental solutions (one from each group). Calcite is known to effervesce in the presence of dilute HCl (10 percent vol/vol), and this test is a common indicator of the presence of calcite in field geological samples. Subsamples of dried corrosion products from experiment tubes NpCSA3 and NpCSB3 were wetted with 10 percent HCl and bubbling or effervescence was clearly observed with the aid of a binocular microscope at low magnification, indicating the presence of calcite. To confirm this finding, additional dried corrosion product material was collected from experiment tubes NpCSB2 and NpCSB3 and submitted for x-ray diffraction analyses in an attempt to definitively identify the presence of calcite. Figure 4-16 shows the results of the x-ray diffraction analysis indicating the presence of calcite in trace amounts.

Table 4-4. Summary of Chemical Analytical Results for Initial Test Cell and Sorption Experiment Solutions

	Experimental Group A				Experimental Group B				Initial Test Cell Mix
Analyte	**NpCSA1**	**NpCSA2**	**NpCSA3**	**NpCSA4**	**NpCSB1**	**NpCSB2**	**NpCSB3**	**NpCSB4**	
pH	9.00	8.98	9.05	9.08	9.14	9.06	9.21	9.19	9.72
Chloride (mg/L*)	55.62	55.99	55.73	55.72	55.53	55.97	55.17	55.53	53.90
Fluoride (mg/L*)	6.40	6.33	6.38	6.37	6.27	6.29	6.30	6.21	6.40
Nitrate (mg/L*)	90.2	91.8	89.2	89.0	83.6	83.8	83.0	83.6	72.2
Sulfate (mg/L*)	23.1	23.1	23.1	22.9	23.2	23.1	22.9	23.0	22.5
Sulfur (mg/L*)	12.28	12.15	12.49	12.38	12.35	12.26	12.37	12.44	12.00
Sodium (mg/L*)	153	150	153	152	159	156	156	157	152
Potassium (mg/L*)	35.5	34.6	34.0	31.2	33.5	34.5	35.3	34.7	33.2
Magnesium (mg/L*)	1.25	1.37	1.20	1.21	1.30	<0.962	<0.983	<0.935	0.938
Calcium (mg/L*)	2.07	2.18	2.02	1.93	1.60	1.47	1.49	1.51	1.01
Boron (mg/L*)	0.867	0.870	0.860	0.886	0.930	0.902	0.886	0.879	0.870
Silicon (mg/L*)	2.53	2.34	2.48	2.45	2.40	2.38	2.32	2.26	2.63

*1 mg/L = 8.35×10^{-6} lb/gal

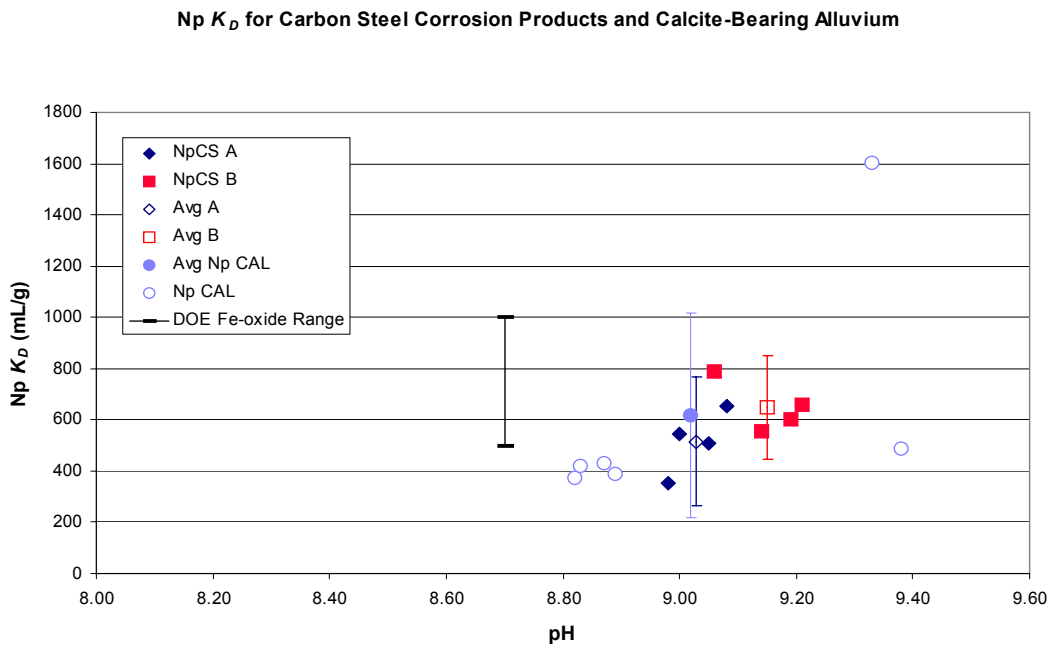

Figure 4-15. Plot of Measured Np-237 K_D Values for the Carbon Steel Corrosion Products, Calcite-Bearing Alluvium, and the Range of Values Used by DOE (Bechtel SAIC Company, LLC, 2004c) for Iron Oxides. The Solid Blue Circle Indicates the Average Measured Np-237 K_D for the Alluvium Samples at High pH; the Error Bars for the Alluvium Represent One Standard Deviation. The DOE Range for Np-237 Sorption onto Iron Oxide Is Not Linked to Any Specific pH Value and Is Shown at pH of 8.7 as an Example Only.

Whether this small amount of calcite is responsible for all or much of the Np-237 sorption in these experiments is unclear, but it is apparent that additional experiments using calcite-free materials will be required to accurately assess the neptunium sorption capacity of the carbon steel corrosion products.

The chemical analyses summarized in Table 4-4 provide other interesting observations. The increase in NO_3^- in the experimental solutions is caused by the addition of NO_3^- within the neptunium spikes, which also produces lower pH values for experimental Group A (whose spike has a higher concentration of HNO_3). Also of note are the results for sulfur and sulfate. If all the measured sulfur was present as sulfate, sulfate concentrations of about 37 mg/L [3.1×10^{-4} lb/gal] would be expected rather than the measured sulfate values of about 23 mg/L [1.9×10^{-4} lb/gal]. So, not only has the initial sulfate concentration decreased from the original simulated pore water solution used to start the test cell experiment [Figure 4.8(m) in Section 4.1.3], but sulfur has increased. The sulfur increase may be a result of contributions from the dissolution of the carbon steel. The cause of the decrease in sulfate is unclear.

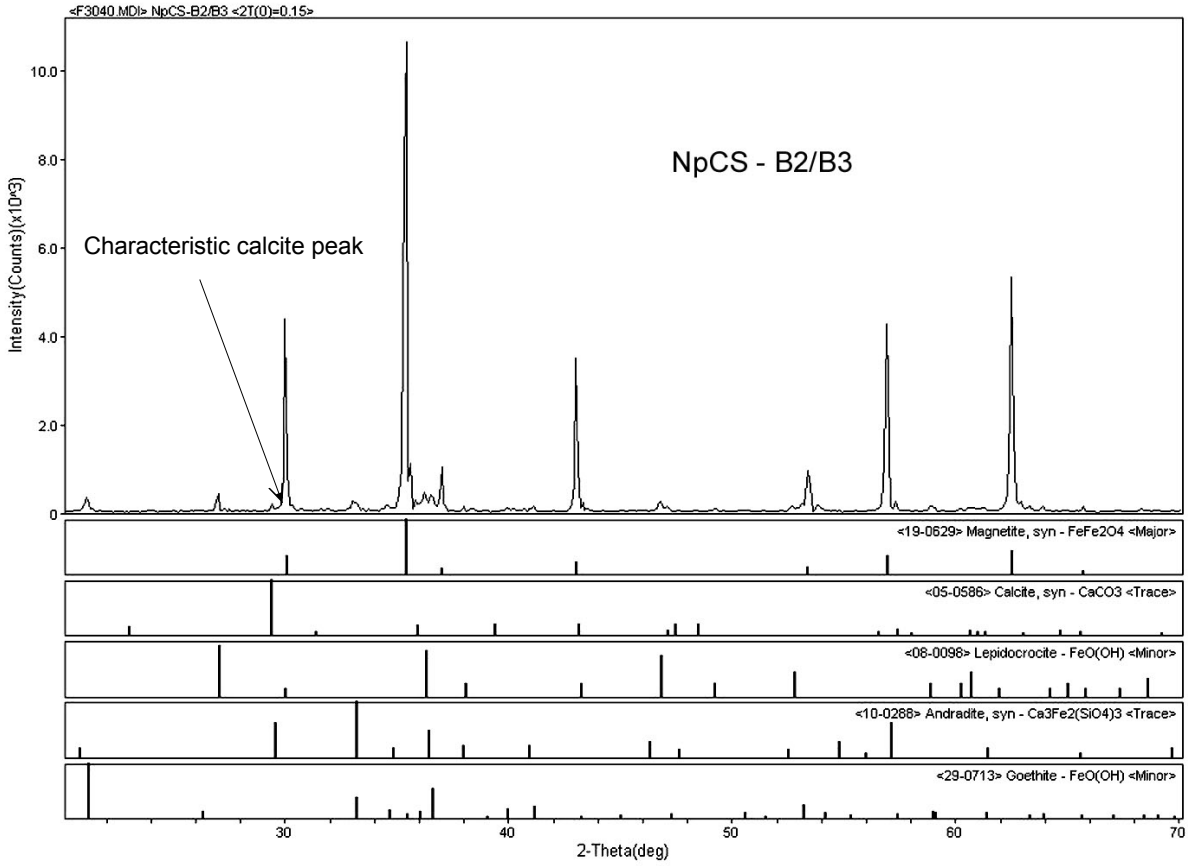

Figure 4-16. X-Ray Diffractogram for Combined Carbon Steel Corrosion Product Samples NpCSB2 and NpCSB3. The Samples Were Dried in Air and Represent the Corrosion Product Substrate after Exposure to Neptunium in the Sorption Experiment. The Small Peak at the Characteristic 2-Theta Value for Calcite Conclusively Identifies the Presence of Calcite in the Sample. Characteristic Peaks for Other Minerals Identified in the Sample Are Also Shown. Although Identified in this Example, the Mineral Andradite Is Likely Not Present in the Sample.

5 SUMMARY, CONCLUSIONS, AND FUTURE WORK

Radionuclide release from the waste package is a complex process that depends upon the corrosion rates of waste package; the chemical composition and flux of groundwater contacting the waste package internal metallic components including 304L, 316L stainless steel, and carbon steel, and the wasteforms; the dissolution rate of high-level waste glass and spent nuclear fuel; the solubility of radionuclides; the availability and stability of colloids; and the retention of radionuclides in secondary phases. Typically, the corrosion rate for carbon steel is significantly higher than for stainless steel or Alloy 22 and has a significant effect on the chemical evolution of the in-package solutions. Furthermore, the pH of the solution is an important parameter that controls the dissolution of wasteforms and determines the speciation of radionuclides between solid and aqueous phases.

5.1 A516 Carbon Steel and Simulated High-Level Waste Glass Immersion

A series of bench-scale experiments was conducted at 60 °C [140 °F] and 90 °C [194 °F] to monitor the evolution of the chemical composition and pH of the fluid inside the waste package for corroding carbon steel and simulated high-level waste glass samples in contact with expected groundwaters. Simulated J–13 Well water and simulated sodium-pore water were used to simulate the expected groundwaters. Results indicated that the corrosion processes increased the pH of the solution from near-neutral to alkaline (pH >9), accompanied by the formation of iron-bearing corrosion product precipitates. The addition of simulated high-level waste glass to the corroding carbon steel solution caused a further increase in pH. Particle size distribution analysis results indicated that the size of most of the corrosion products is in the micrometer range. The content of colloid-sized particles {< 1 μm [0.04 mil]} appeared to be low; however, the ability to accurately measure colloidal concentration may be limited by the resolution of the particle-sized analyzer used in this work. The apparently low colloid content is unlikely to be an ionic strength effect, as the experimental solutions were near or below an ionic strength of 0.01 molal. The upper limit of the range of point of zero charge values for iron oxides and oxyhydroxides is about pH 8.8 (Langmuir, 1997), which is lower than experimental values. Thus, the low colloid content is not clearly related to coagulation resulting from diminished particle repulsion, though this may have an effect. The pH increases are in contrast to the U.S. Department of Energy (DOE) proposed model abstraction for in-package chemistry for Yucca Mountain in which the pH is expected to remain near neutral after initial acidic conditions (pH around 4). The measured corrosion rates of carbon steel were lower than those used by DOE in the in-package chemistry model.

5.2 Np-Sorption Experiments

Limited neptunium-sorption tests were performed to assess the capability of carbon steel corrosion products to sorb radionuclides. Carbon steel corrosion products showed substantial sorption of neptunium; however, a very small amount of calcite was identified in the corrosion products, which could also contribute to significant neptunium-sorption. The presence of calcite within the corrosion products makes it difficult to definitively assign the sorption of neptunium to the corrosion products.

5.3 Future Work

The results presented in this report are preliminary, and most laboratory tests only deal with carbon steel. In the waste package design, DOE may use stainless steel to eliminate carbon steel. Typically, the corrosion rate of carbon steel is significantly higher than stainless steel and the pH change observed in this work may not be applicable to stainless steel. In addition, the pH changes observed may not be solely due to carbon steel corrosion. Chemical composition analysis of the solution after the immersion of carbon steel showed that glass from the test cell dissolved into the solution, KCl from the pH probe leached into the solution, and calcium and magnesium precipitated from the solution. These factors may also contribute to pH changes of the solution. Preliminary Center for Nuclear Waste Regulatory Analyses modeling has not identified the pH-controlling mechanism in laboratory tests. X-ray diffraction analysis of the corrosion products detected trace amounts of calcite, which makes neptunium sorption on corrosion products inconclusive. Future work will focus on the following areas:

- Conduct immersion tests of stainless steel specimens in simulated sodium-pore water at 60 °C [140 °F], monitor accompanying pH and chemical composition changes, and detect the presence of colloids due to stainless steel corrosion. In parallel, set up a test with simulated sodium-pore water only under the same conditions with the same test cell in order to pinpoint the pH changes due to glass dissolution from the test cell, KCl leaching from the pH probe, calcium and magnesium precipitation from solution, and chemical equilibrium perturbation by removing samples for chemical analyses and replacing them with the original test solution.

- Study the corrosion products of carbon steel and stainless steel using *in-situ* Raman spectroscopy.

- Install an O_2 probe in the test cell to determine whether the O_2 fugacity is reduced.

- Prepare a solution with a reduced amount of Ca^{2+} to avoid calcite precipitation, and repeat the carbon steel immersion tests in such a solution to produce corrosion products. Conduct neptunium-sorption tests on these corrosion products to determine the effect of calcite on sorption.

- Continue the efforts to model the chemical evolution of the experimental solutions on steel corrosion. In addition, construct other single- and multi-component models for aqueous chemical evolution in order to evaluate the DOE results.

- Replace carbon steel with stainless steel in the simulations to investigate chemical effects of potential waste package design changes.

- Improve the method of identifying iron colloids.

6 REFERENCES

ASM International. *Corrosion*. Volume 13 of Metals Handbook. 9th Edition. Metals Park, Ohio: ASM International. 1987.

Bechtel SAIC Company, LLC. "Technical Basis Document No. 7: In-Package Environment and Waste Form Degradation and Solubility." Rev. 1. Las Vegas, Nevada: Bechtel SAIC Company, LLC. 2004a.

———. "In-Package Chemistry Abstraction." ANL–EBS–MD–000037. Rev. 3. Las Vegas, Nevada: Bechtel SAIC Company, LLC. 2004b.

———. "EBS Radionuclide Transport Abstraction." ANL–WIS–PA-000001. Rev. 1. Las Vegas, Nevada: Bechtel SAIC Company, LLC. 2004c.

———. "Engineered Barrier System: Physical and Chemical Environment Model." ANL–EBS–MD-000033. Rev. 2. Las Vegas, Nevada: Bechtel SAIC Company, LLC. 2004d.

———. "Geochemistry Model Validation Report: Material Degradation and Release Model." Rev. 0. Las Vegas, Nevada: Bechtel SAIC Company, LLC. 2001.

Bertetti, F.P. "Laboratory and Modeling Studies of Neptunium Uptake on Calcite." San Antonio, Texas: CNWRA. 2002.

Bertetti, F.P. and B. Werling. "Sorption of Neptunium-237 on Alluvium Collected from Fortymile Wash, Nye County, Nevada—Status Report." San Antonio, Texas: CNWRA. 2005.

Dunn, D.S., M.B. Bogart, C.S. Brossia, and G.A. Cragnolino. "Corrosion of Iron Under Alternating Wet and Dry Conditions." *Corrosion*. Vol. 56, No. 5. pp. 470–481. 2000.

Dzombak, D.A. and F.M.M. Morel. *Surface Complexation Modeling: Hydrous Ferric Oxide*. New York, New York: John Wiley and Sons. 1990.

Langmuir, D. "Aqueous Environmental Geochemistry." Upper Saddle River, New Jersey: Prentice Hall. 1997.

NRC. "Risk Insights Baseline Report." ML040560162. Washington, DC: NRC. April 2004a. <www.nrc.gov/waste/hlw-disposal/reg-initiatives/resolve-key-tech-issues.html>

———. "Review by the U.S. Nuclear Regulatory Commission Office of Nuclear Material Safety and Safeguards of the U.S. Department of Energy Agreement Responses Related to the Potential Geologic Repository at Yucca Mountain, Nevada: Key Technical Issue Agreements CLST.3.03, CLST.3.03 AIN–1, CLST.3.04, CLST.3.04 AIN–1, CLST.3.06, CLST.3.06 AIN–1, CLST.3.07, CLST.3.08, CLST.3.08 AIN–1, CLST.3.09, CLST.3.09 AIN–1, ENFE.3.03, TSPAI.3.08, TSPAI.3.14, GEN.1.01 Comment 116, GEN.1.01 Comment 124, DOE Initial Response to GEN.1.01 Comment 124, and GEN.1.01 Comment 126." ML043490209. Washington, DC: NRC. 2004b.

———. "Review by the U.S. Nuclear Regulatory Commission Office of Nuclear Material Safety and Safeguards of the U.S. Department of Energy Responses Related to the Proposed Geologic Repository at Yucca Mountain, Nevada: Key Technical Issue Agreements CLST.3.02, ENFE.3.04, and CLST.3.05." ML043490031. Washington, DC: NRC. 2004c.

Nugent, M. and D.R. Turner. "Preliminary Determination of the Effect of Calcite Growth Rate on Neptunium Uptake by Coprecipitation With Calcite—Letter Report." San Antonio, Texas: CNWRA. 2000.

Pourbaix, M. *Atlas of Electrochemical Equilibria in Aqueous Solutions*. Vol. 1. Toronto, Canada: Pergamon Press. 1996.

Wolery, T.J. "EQ3/6, A Software Package for Geochemical Modeling of Aqueous Systems: Package Overview and Installation Guide (Version 7.0)." UCRL–MA–110662–PT–I. Livermore, California: Lawrence Livermore National Laboratory. 1992.

Zarrabi, K., S. McMillan, S. Elkonz, and J. Cizdziel. "Corrosion and Mass Transport Processes in Carbon Steel Miniature Waste Packages." TR–03–003. Rev. 0. Las Vegas, Nevada: University and Community College System of Nevada. 2003.